

Validation of the MVMA/HSRI Phase II  
Straight Truck Directional Response  
Simulation  
MVMA Project #1.29  
The Univ. of Michigan, HSRI, Oct., 1978

EDC Library Reference No. 1071



UM-HSRI-78-46

HSRI  
42575

VALIDATION OF THE MVMA/HSRI PHASE II  
STRAIGHT TRUCK DIRECTIONAL RESPONSE  
SIMULATION

MVMA Project #1.29

Final Technical Report  
Motor Truck Braking and Handling Performance Study

Thomas D. Gillespie

October 1978

Highway Safety Research Institute  
The University of Michigan  
Ann Arbor, Michigan 48109



42575

## Technical Report Documentation Page

1. Report No. UM-HSRI-78-46	2. Government Accession No.	3. Recipient's Catalog No.	
4. Title and Subtitle VALIDATION OF THE MVMA/HSRI PHASE II STRAIGHT TRUCK DIRECTIONAL RESPONSE SIMULATION		5. Report Date October 1978	
		6. Performing Organization Code	
7. Author(s) T.D. Gillespie		8. Performing Organization Report No. UM-HSRI-78-46	
9. Performing Organization Name and Address Highway Safety Research Institute The University of Michigan Huron Parkway & Baxter Road Ann Arbor, Michigan		10. Work Unit No. 361292	
		11. Contract or Grant No. MVMA Proj. #1.29	
12. Sponsoring Agency Name and Address Motor Vehicle Manufacturers Association 320 New Center Building Detroit, Michigan 48202		13. Type of Report and Period Covered Final	
		14. Sponsoring Agency Code	
15. Supplementary Notes			
16. Abstract Validation tests of the MVMA/HSRI straight truck directional response computer simulation program were conducted. A three-axle straight truck was instrumented and operated through test maneuvers both empty and loaded to 44,500 lb gross vehicle weight. Constant radius, steady-state cornering tests were run over a range of speeds up to limit cornering levels. Step-steer transient tests to beyond the vehicle stability limit were also performed. Computer simulations of the test maneuvers were compared against the measured response of the test vehicle. The simulation exhibited good agreement with the experimental results in prediction of low-speed cornering, understeer characteristics and transient response. Disparities in the validation due to lack of tire relaxation length and steering system compliance models in the computer simulation were noted.			
17. Key Words Computer simulation, validation, truck cornering, truck stability limits, truck directional response		18. Distribution Statement UNLIMITED	
19. Security Classif. (of this report) NONE	20. Security Classif. (of this page) NONE	21. No. of Pages	22. Price



## TABLE OF CONTENTS

1.	INTRODUCTION. . . . .	1
2.	BACKGROUND. . . . .	2
3.	APPROACH. . . . .	4
4.	TEST PROGRAM. . . . .	5
	4.1 Parameter Measurement. . . . .	5
	4.2 Instrumentation and Safety Equipment . . . . .	12
	4.3 Testing. . . . .	14
5.	VALIDATION. . . . .	17
	5.1 Low-Speed Cornering. . . . .	17
	5.2 Steady-State Cornering . . . . .	19
	5.3 Transient Maneuvers. . . . .	24
6.	CONCLUSIONS AND RECOMMENDATIONS . . . . .	34
7.	REFERENCES. . . . .	36
APPENDIX A:	Copy of "Survey of Single-Axle Steering and Suspension Properties - MVMA Project 1.31," Third Quarterly Report, January-March 1977. . . . .	37
APPENDIX B:	Test Vehicle Data Input List. . . . .	52





## 1.0 INTRODUCTION

In the 1977 fiscal year, the Motor Vehicle Manufacturers' Association (MVMA) granted support for further research on the validity of the MVMA/HSRI Phase II Straight Truck Directional Response Simulation in predicting directional response behavior. The work was supported as a part of the continuing research program on "Motor Truck Braking and Handling Study" begun in 1971; and was complementary to other planned programs which in total will eventually evaluate the validity of tractor-trailer directional response simulation and simulation of combined braking and steering maneuvers.

The specific objective of the study reported herein was to test a suitably instrumented straight truck, measure the vehicle properties necessary to describe it for simulation purposes, and perform simulations of the test maneuvers to compare predictions of the computer model to the actual vehicle behavior.

## 2.0 BACKGROUND

The objective of the "Motor Truck Braking and Handling Study" begun in 1971 was development of methodology for predicting how trucks and tractor-trailers respond to driver-initiated steering and braking inputs as tools for evaluating new and existing vehicle designs in their ability to meet given performance specifications. The research focused on three areas:

- Developing mathematical descriptions of motor truck systems which were assembled into computer programs representing simulations of the total vehicle.
- Developing methodology and hardware for measuring vehicle properties necessary to describe the vehicle in a simulation process.
- Comparing the performance of actual vehicles to the calculated results from computer simulation models as a test of the validity of the simulations developed.

The major products of the Motor Truck Braking and Handling Study emerged as computer simulation programs reflecting the state of development at each of three phases in the research. Phase I, ending in 1972, produced a mathematical model of the straight-line braking performance of trucks and tractor-trailers [1]\*. The braking model represented the vehicle in the pitch plane with up to 15 degrees of freedom for a five-axle tractor-semitrailer, and emphasized modeling of the tire/wheel/brake system. The Phase I program was the basis for development in 1973 of a Phase II directional response simulation, of interest here, and an improved Phase III braking simulation model [2] in 1976.

---

\*Numbers in brackets denote references at end.

The Phase II simulation model [3] was developed from the Phase I model by expansion of the program to include motions in the yaw and roll degrees of freedom, development of tire lateral force models and modeling of the roll-dependent steering and moment properties of axle/suspension systems. A major aspect of that research was devoted to investigation of vehicle properties influencing directional response, culminating in a validation study of the Phase II simulation model.

Validation at that time was based on two vehicles—a 50,000-lb GVW, three-axle straight truck and a 46,000-lb GVW, three-axle tractor/40-foot trailer combination. The tests performed were steady-state turning (fixed steer angle) and braking in a turn. With a few exceptions with the tractor-trailer, the measured results and the predicted results were in very close agreement.

Nevertheless, in the intervening years, as research on truck handling continued and changes were made in the tire model, the need for a second validation exercise arose. This report covers the second validation of the straight-truck directional-response simulation conducted in 1977-78.

### 3.0 APPROACH

In this second validation, the adopted intent was to do more than simply compare calculations from the directional response simulation against test results for another vehicle. Rather, in designing the project the choice was made to look at validation from a broad perspective in which the function of directional response simulation is seen as the ability to predict the relationship between steering inputs and vehicle response over an extensive range of maneuver levels, be they steady-state or transient. In this light, the areas in which validation needed critical testing were identified as follows:

- Low speed cornering - evaluating the prediction of Ackermann steer angles as tests of the geometric accuracy of the modeling equations, and the effects of tandem axles.
- Steady-state, high-speed cornering - evaluating the change in lateral forces produced at each axle (understeer gradient) as lateral acceleration levels are increased up to the limits of vehicle cornering.
- Transient response - evaluating the modeling of the yaw and roll inertial effects that determine initial response to steering inputs.

Basically, the first two areas are tests of modeling of the primary factors determining directional response—the tire lateral forces developed as a result of slip angle and load, the overall factors determining slip angle (gross vehicle motions, roll steer effects, etc.), and the overall factors determining load (vehicle static load and roll effects as transmitted through the suspensions and axles). The remaining elements of the vehicle modeling are tested in the transient response—i.e., the inertial response in the yaw plane resulting from time-dependent lateral forces and the inertial response in roll with the dependent effects on axle roll steer and side-to-side load transfer.

## 4.0 TEST PROGRAM

For the testing program, a three-axle truck-tractor on hand at the Institute was selected as the test vehicle. The relevant specifications of the vehicle are given below.

### Specifications of the Test Vehicle

- 1967 IHC Model COF-4000 D
- COE with sleeper, 83" BBC
- 142" wheelbase
- 12,000 lb, I-beam front axle with 54" semi-elliptical steel leaf suspension
- RA-335 38,000 lb, rear axles with air spring suspension
- 10.00x22 Firestone Transport 1 tires
- 8V71N Detroit Diesel engine
- RT0 915 Roadranger transmission
- S-44 manual steering gear
- 45,000 lb gross vehicle weight rating

The vehicle was prepared by inspection of the steering and suspension systems, installation of a load bed, and mounting new tires all around.

### 4.1 Parameter Measurement

The vehicle was put through a series of parameter measurements to determine the properties needed as input for the simulation. After weighing the vehicle to determine the curb weights at front and rear axles, the vehicle was placed on the pitch plane swing to determine the

sprung mass center of gravity (c.g.) location and pitch moment of inertia. The yaw and roll moments of inertia were then estimated based on these measurements, and suggested methods for estimating vehicle inertial properties [4]. In order to determine the unsprung masses of each axle, each axle was, in turn, partially disconnected from the chassis and suspended by a load cell. (Completely removing each axle is a more accurate method but involves substantially greater effort to remove steering linkages, drivelines, etc., and then to realign and reinstall the axle. In light of the noncritical nature of unsprung mass values in determination of directional behavior, the additional effort is usually unjustified.) Figure 1 shows the nature of the results for the rear axles when the air springs and shock absorbers are removed, leaving only the driveline and trailing arms connected. The axle is lifted and lowered to display the coulomb friction and residual spring rate in the linkages still connected and the weight is determined at the normal ride height position.

With the unsprung weights known, the roll moment of inertia for the axles was estimated by calculation, since this parameter is likewise not critical to directional response behavior. For the estimate, a "barbell" model of the axle was assumed with the moment of inertia determined from the assumed mass distribution. For the front axle, the mass is assumed to be distributed 20% in the axle and 80% in the wheels. For the rear axles, the mass is assumed distributed as 60% in the axle assembly (of which one-half is considered a point mass at the center and one-half is uniformly distributed along the axle) and the remaining 40% is allocated as mass of the wheels.

The determination of suspension parameters was made from measurements on the suspension parameter measurement facility [5]. The properties measured and reported in that reference were:

- 1) Vertical spring rate and hysteresis characteristics
- 2) Roll stiffness and hysteresis characteristics
- 3) Roll center position

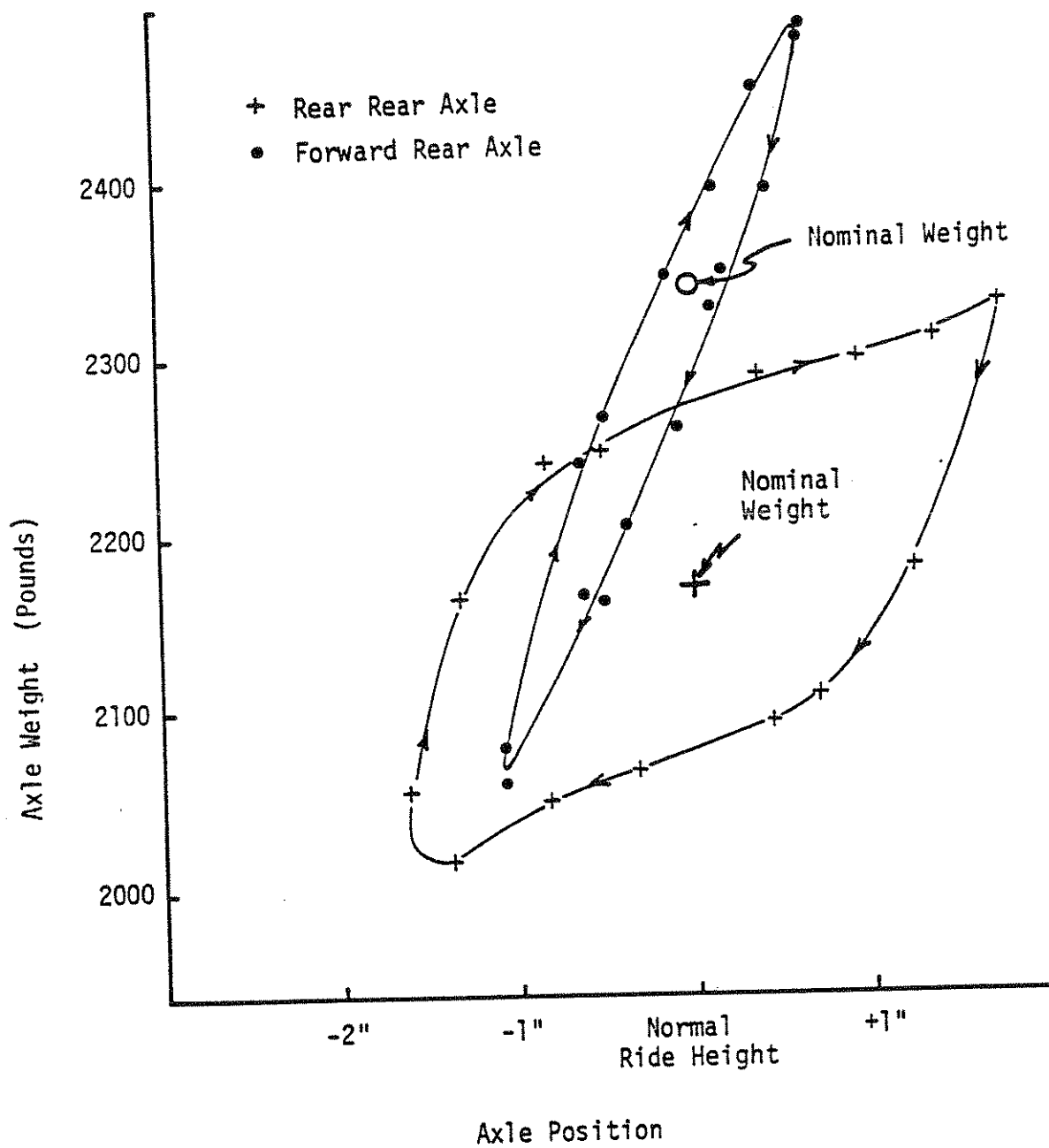


Figure 1 Truck Rear Axle Weight Measurements.

- 4) Roll steer properties
- 5) Bounce steer properties
- 6) Compliance steer response to aligning moment
- 7) Compliance steer response to brake force
- 8) Overall steering ratio

A copy of that report is included as Appendix A to this report.

The rear suspension parameters were measured on the same facility. Only the rearmost axle was measured. The rearmost axle on this vehicle is rigidly clamped to the trailing arms, resulting in a roll stiffness effect which is not duplicated on the forward rear axle which has pin joint connections to the trailing arms. The forward rear axle roll stiffness thus derives entirely from the spring rate and spring spacing and is duplicated in the simulation by input of those parameters. The parameters measured on the rear axle were:

- 1) Vertical spring rate and hysteresis characteristics
- 2) Roll stiffness and hysteresis characteristics
- 3) Roll steer properties
- 4) Bounce steer properties

Bounce steer effects were negligible. Figures 2, 3, and 4 show results obtained for the other three properties.

One of the most essential parameters required for describing the vehicle are the tire properties. The properties of the tires used on the vehicle were measured at the actual test site with the Institute's Mobile Tire Dynamometer [6]. Measurements of the lateral force and aligning torque over a range of five slip angles and five loads were obtained.

The remaining parameter measurements were primarily geometric measurements such as wheelbase, track width of front and rear axles, lateral distance between springs, dual tire spacings, etc. A complete list of the computer input data for the vehicle is included as Appendix B.



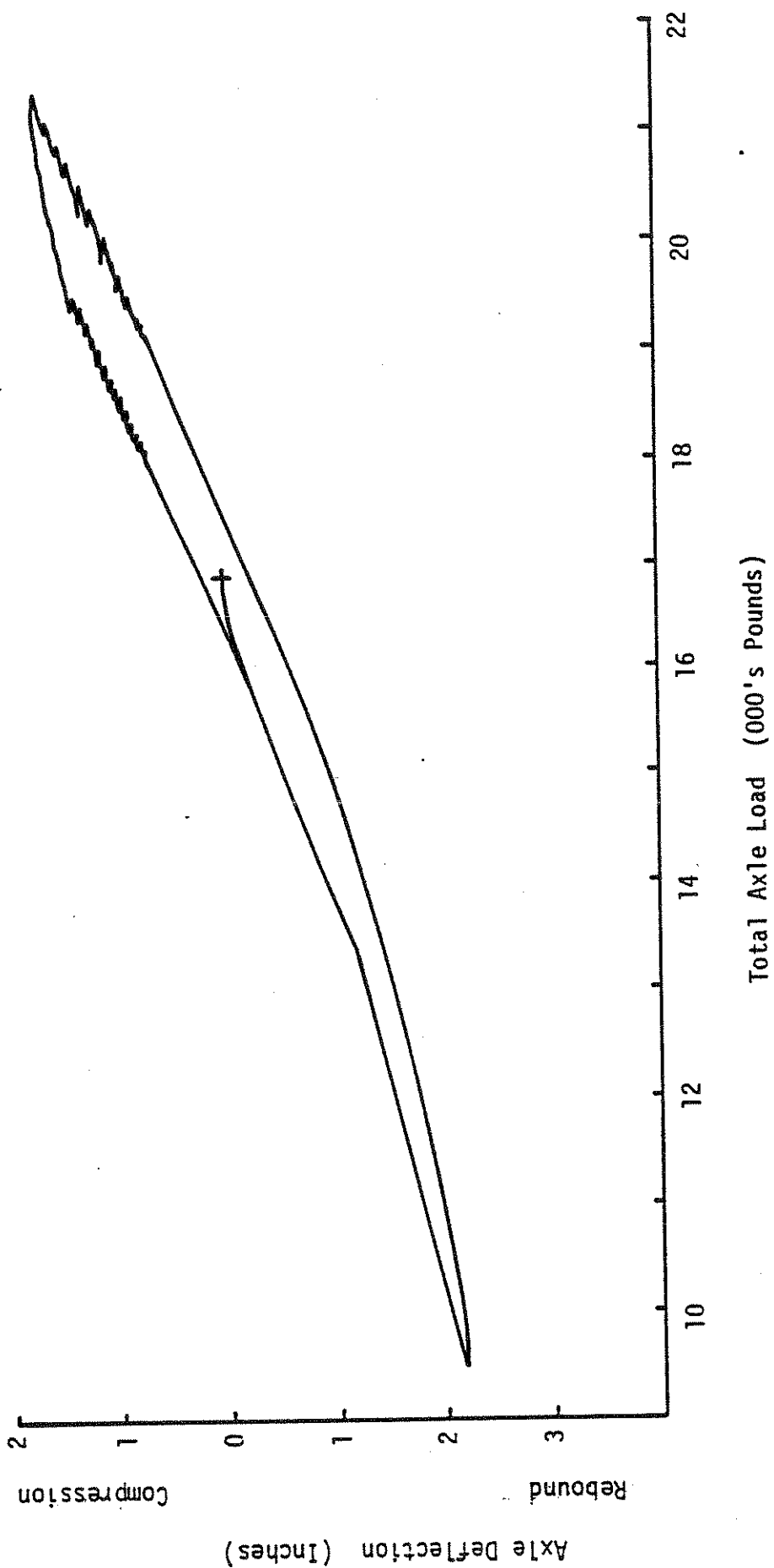


Figure 2. Test Vehicle Rear Axle Spring Rate.

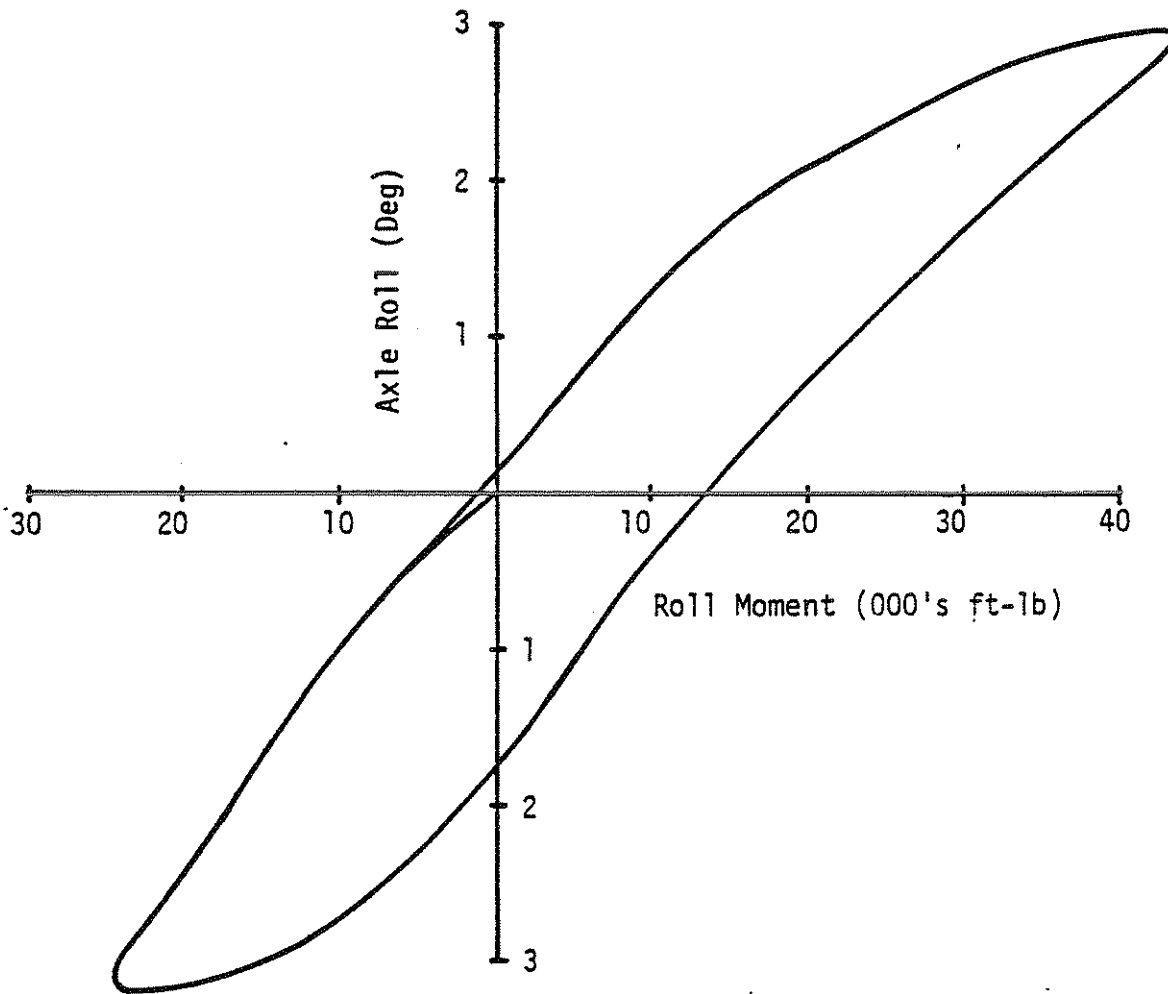


Figure 3. Test Vehicle Rear Axle Roll Stiffness

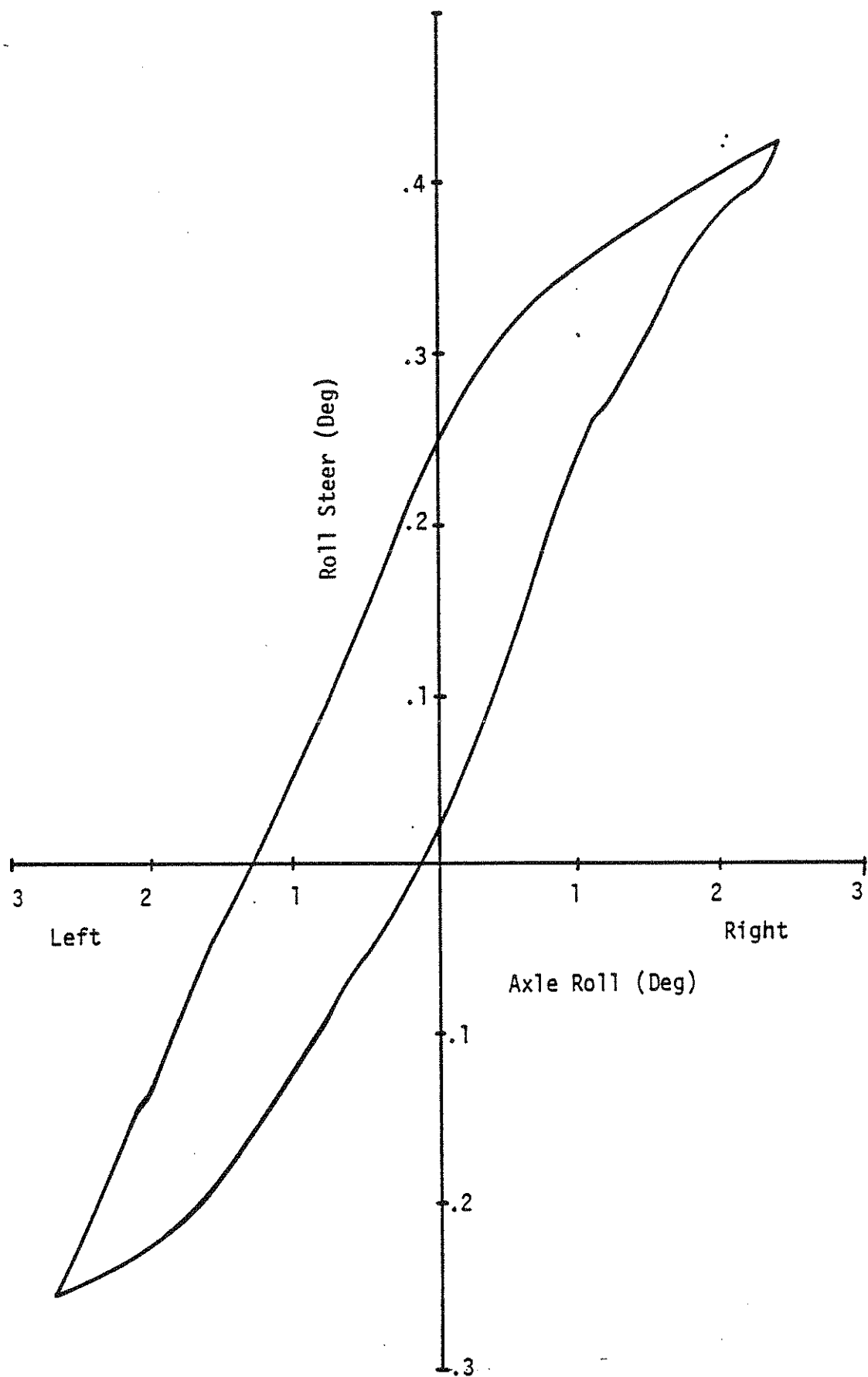


Figure 4. Test Vehicle Rear Axle Roll Steer Characteristics

#### 4.2 Instrumentation and Safety Equipment

After parameter measurement, the vehicle was prepared for testing by installation of safety equipment and instrumentation.

The vehicle, as available, included only the chassis and a steel flat-bed. Since limit maneuvers were to be attempted, a rollbar and rollover outriggers were considered essential equipment. The combined rollbar-outrigger assembly, shown in Figure 5, was designed, built, and installed on the vehicle. The main rollbar element is fabricated from six-inch schedule 40 pipe built to the general outline of the cab. The rollbar and associated braces serve also as attachment points for a three-leg outrigger brace. The outrigger foot is a 20-inch convex skid plate which contacts the pavement. The top brace of the outrigger includes ball ends screwed into the brace to allow adjustment of the outrigger height over the range of 0-2 feet of ground clearance. The top brace is fastened by a pin connection at the outrigger foot so it can be disconnected and swung up onto the load bed for vehicle transit. A hand-operated winch raises the remainder of the outrigger into the vertical position fitting within a 96-inch overall width for highway travel.

The outrigger system was used throughout all testing with satisfactory results. Outrigger touchdown occurred on numerous maneuvers, and was quite severe on one occasion. In those maneuvers, it adequately stabilized the vehicle to allow recovery from the maneuver and caused no observable pavement damage.

The instrumentation package installed for the testing consisted of transducers, conditioning amplifiers, and an FM magnetic tape recorder. The transducers installed were:

- Fifth wheel speed transducer
- Yaw rate gyro
- Roll rate gyro
- Steering-wheel angle transducer
- Right road-wheel angle transducer

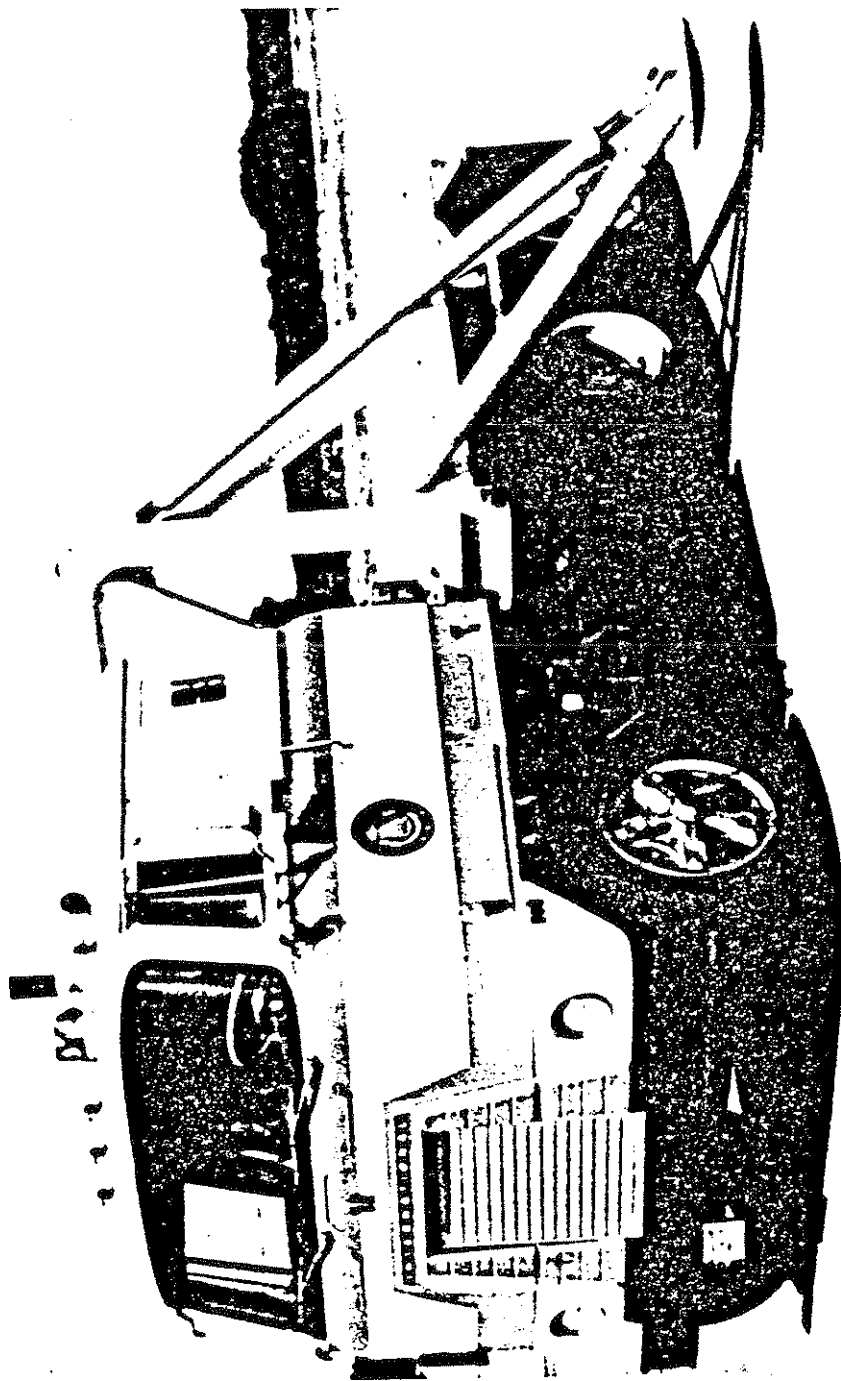


Figure 5 Rollbar-Outtrigger Assembly on the Test Vehicle

The speed, yaw rate, and roll rate transducers are routine instrumentation. The steering-wheel angle transducer was a component of a steering-wheel limiter system fabricated to allow steering-wheel inputs to preselected values. The steering-wheel limiter shown in Figure 6 was based on hardware developed at the Institute under NHTSA sponsorship [7]. Modifications were made to allow installation of a 21-inch truck steering wheel and the limiting pin was modified to include a spring release so that the limiting function could be defeated with a touch of the release lever should the vehicle get out of control. Steering-wheel angle is measured by a multi-turn potentiometer built into the steering limiter and geared directly to the steering shaft.

Growing concerns with the potential influence of steering system compliance in the directional response of heavy vehicles [8], especially as a factor in the understeer gradient, were cause for the addition of a road-wheel angle transducer. The angle was transduced by a string potentiometer installed on the axle and connected to the leading edge of the brake backing plate.

The steering system and transducers were then calibrated by placing the front wheels on a steer angle turntable and exercising the steering system through the expected range of travel.

#### 4.3 Testing

The vehicle was tested empty (with flat-bed, rollbar, and outriggers installed) and loaded to a 44,500-lb gross vehicle weight. Loading was accomplished with cast steel weights stacked to raise the sprung mass center of gravity from 48 inches to 62-1/4 inches above the ground. The tests were conducted at the Chrysler Corporation's Chelsea Proving Grounds on the Vehicle Dynamics Test Facility, consisting of a 2-1/2-mile oval enclosing an 800-foot square asphalt pad. Circles of 50-, 100-, and 250-foot radius were laid out and marked on the pad, along with 500-foot radius arcs tangent to the approaches.

Each circle was marked with cone-type delineators and the vehicle was driven at constant speed on each circle, with speeds ranging from

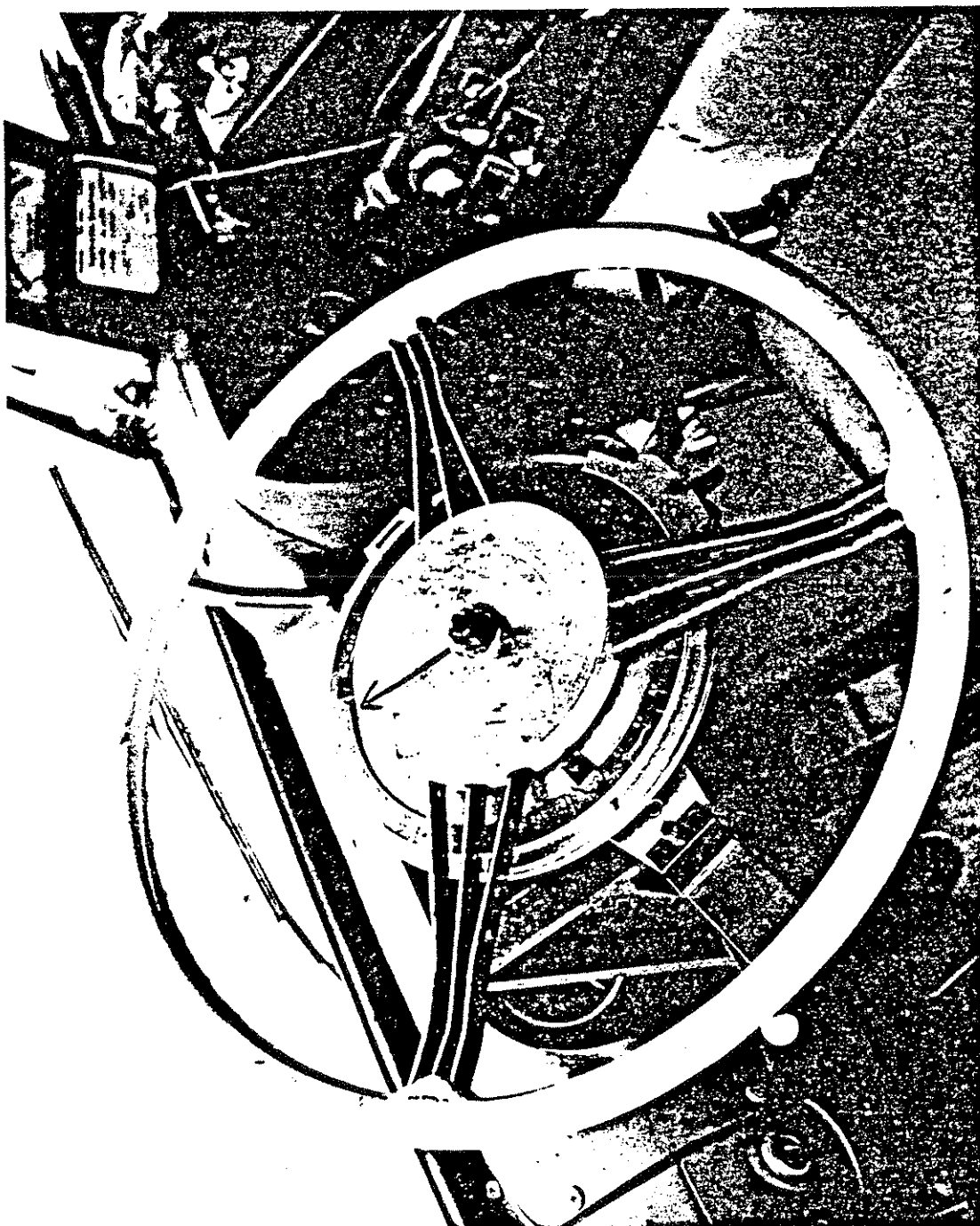


Figure 6 Photograph of the Steering Wheel Limiter

a few miles per hour to the maximum possible. The recorded data was analyzed at the Institute to determine the average steering-wheel and road-wheel angle at each condition. At the completion of each test, the vehicle was steered to the straight-ahead direction and stopped so that a brief roll rate record was obtained for integration to obtain the roll angle during test.

Transient tests of the step-steer type were conducted at 20 and 50 miles per hour. The steering-wheel limiter was preset to selected limits and, as the vehicle entered the skid pad from the approach roads, left or right steer inputs were applied. Steer inputs to levels beyond the limits of vehicle stability were applied. In such maneuvers, the vehicle became yaw divergent with ever increasing sideslip, yaw rate, and roll angle until such time that outrigger touchdown would occur and recovery would be initiated.

All told, approximately 200 tests were performed.



## 5.0 VALIDATION

At the completion of testing, runs were conducted with the Phase II straight truck directional response simulation of the test vehicle to evaluate the degree of agreement between the simulation and experimental results. The agreement was examined in the areas of validation discussed in Section 3.0—low-speed cornering; steady-state, high-speed cornering; and the transient maneuvers.

### 5.1 Low-Speed Cornering

For two-axle vehicles, low-speed cornering is dependent only on geometry from which derives the Ackermann angle. For heavy trucks with tandem axles and dual tires, the axles must scrub even during low-speed cornering and, hence, dependence on tire stiffness parameters can be expected, i.e.:

$$\delta = \frac{1}{R} \cdot WB \cdot f(\text{axle loads, tire stiffness, axle geometry})$$

where

$\delta$  = steer angle (rad)

$\frac{1}{R}$  = path curvature (1/ft)

WB = wheelbase (ft)

Figure 7 shows the relationship between front-wheel steer angle and path curvature for the empty and loaded truck as determined experimentally on 50-, 100-, 250-, and 500-foot radius turns, and as predicted by the simulation. The experimental values are shown as the data points and are plotted at the given radius plus the half-width of the truck, since it was run on a radius just outside of the cones delineating the given radius. The simulation predictions are shown as the lines which are linear and are established by running the simulation at several values of steer angle over the range and noting the steady-state radius of turn.

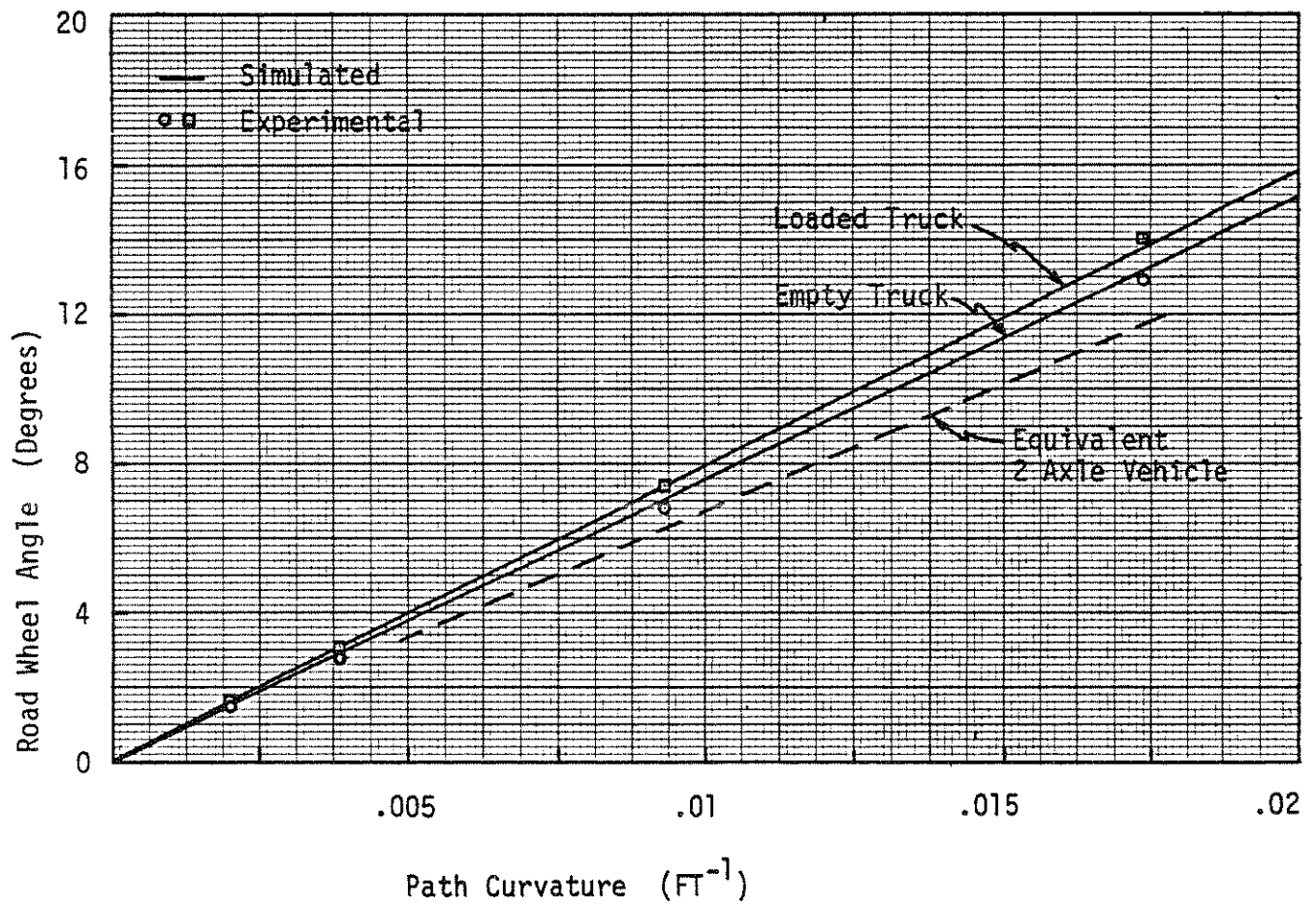


Figure 7 Comparison of Experimental and Simulated Results for Low Speed Cornering

Excellent agreement is obtained. To show the relative magnitude of the tire scrub effects with tandem-axle vehicles, a broken line representing the turning of a two-axle vehicle of the same wheelbase is shown. The effects which are nominally of a 10% relative magnitude are thus simulated quite accurately in the program.

It is worth noting that additional analysis was performed to verify this effect and to evaluate the most significant causative factors [9]. Tandem-axle scrub, which is modeled in detail in the simulation, was found to be the dominant cause. Dual-tire aligning moments (the moment arising from the two tires rolling at the same speed on paths of different radius), which is not included in the model, fortunately turned out to have an insignificant effect.

Aside from the implications relating to validation of the computer program, the reader might find the above discussion of interest with regard to predicting the maneuverability of a vehicle. Manufacturers often specify a curb-to-curb turning diameter for a vehicle as one of the specifications to be considered by potential customers. For three-axle heavy vehicles, the turning diameter is not solely dependent on the Ackermann steer angles (hence, maximum wheel cut and wheelbase), but also on the tires, tandem geometry, and the vehicle load conditions. Thus the computer simulation (or, alternatively, the analytical solution given in Reference [9]) may be considered as a means to predict minimum turning diameter for various vehicle combinations in lieu of experimental tests or the less accurate Ackermann steer calculations.

## 5.2 Steady-State Cornering

As speed and, hence, lateral acceleration, builds up, the cornering behavior of a vehicle changes with the build-up of increasing slip angles at the front and rear axles. Comparing the understeer gradients of a simulation against that of an actual vehicle represents a very critical test because the understeer gradient depends not so much on the ability to calculate the absolute values of lateral force generated at each axle, but on the differences between the lateral forces calculated

for the front and rear axles. The accuracy of experimentally measured understeer gradients is often questioned because of the variability of gradients measured on the same vehicle at different test sites. Nevertheless, the fact that the tire characteristics were measured on the site where testing was performed would be expected to eliminate some of those sources of variation.

The understeer characteristics of the empty and loaded vehicle were determined from the constant speed/constant radius tests. For each test, the average steer angle (road wheel and steering wheel) was determined from the recorded measurements. Then for each radius, the change in steer angle (from the low speed steer angle) was determined as a function of lateral acceleration. The gradient of steer angle with lateral acceleration is defined as the understeer gradient.

Understeer tests with the simulation were performed by conducting runs at constant steer angle of several different levels. When the simulation vehicle reached near steady state, the radius of turn, lateral acceleration, and steer angle was noted. For the radius of turn achieved, the low-speed steer angle was determined by the methods described in the preceding section. Thence, the change in steer angle (run steer angle minus low-speed steer angle) was obtained.

Figure 8 shows the observed behavior for the loaded truck. The upper plot shows the change in road-wheel steer angle as a function of lateral acceleration; the data points represent experimental test values and the curve is obtained from a number of simulation runs. Again, good agreement is obtained. Both simulation and experiment indicate a nominal zero degree/g understeer at low lateral acceleration levels, with negative trends (oversteer) at higher levels. The experimental data points extend only to the 1/3 g level because the vehicle became too unstable at that point to permit higher level tests. Likewise, the simulation evidences instability at the same level, resulting in lift-off of the inside rear wheels.

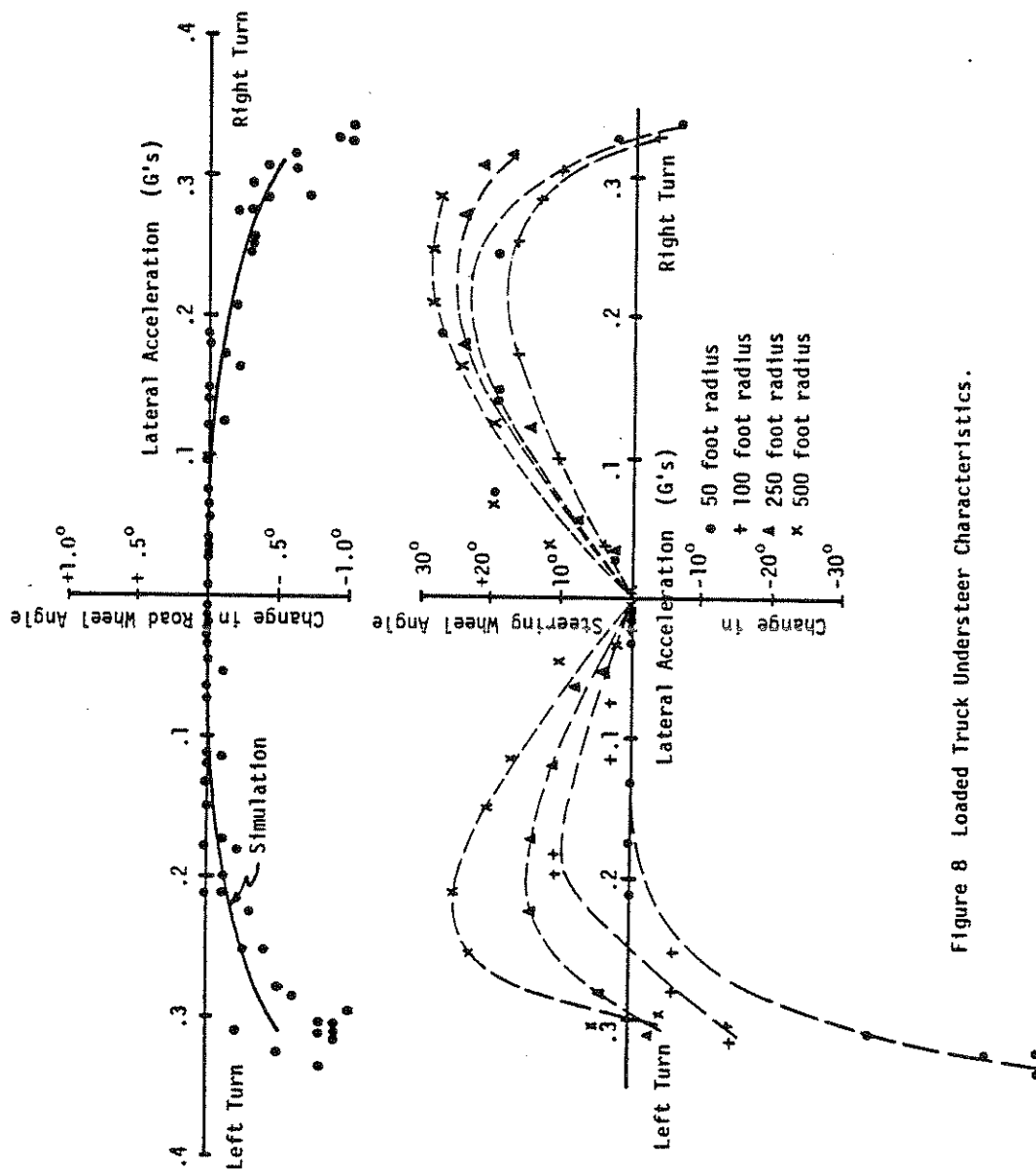


Figure 8 Loaded Truck Understeer Characteristics.

The bottom plot shows the understeer characteristics measured at the steering wheel. The simulation does not determine steering-wheel angles, however, this plot is included to show the significant influences of steering system characteristics on the handling of the vehicle. Though the understeer effects are nearly symmetric left and right at the road wheel, at the steering wheel the effects are dependent on radius of turn and considerable asymmetry is observed. For right-hand turns for which the left road wheel produces most of the effort, relatively consistent performance is observed. For left-hand turns for which the right road wheel produces most of the effort, the radius of curvature influences the behavior. The probable causes of the asymmetry are the differences in the roll steer properties right and left and the difference in compliance between the steering wheel and the left and right road wheels, respectively.

The plots of roll steer effects shown in Figure 6 of Appendix A show a definite asymmetric roll steer characteristic with the greatest range of variability in the right-hand roll/left-hand steer situation (the left turn portion of the plot in Figure 8). The roll steer coefficient is zero at  $13^\circ$  left road wheel angle, equivalent to the 50-foot radius turns, hence, the understeer gradient at the steering wheel and road wheel are understandably the same. On the other hand, near zero degrees road-wheel angle, a roll steer effect equivalent to understeer, is evident from Figure 6 of Appendix A. Thus, an understeer effect at the steering wheel would be expected at the large radius turns, such as 500 feet. Though the observed roll steer and understeer characteristics of the vehicle are in qualitative agreement, the numerical values are not accurate enough to allow deeper analysis of the physical mechanisms involved.

The understeer characteristics of the empty truck were measured as well, and are shown in Figure 9. Again, good agreement between the vehicle tests (data points) and the simulation were obtained in the upper plot. A slight asymmetry of the empty truck behavior is evident, which does not show up in the simulation. The understeer characteristics measured relative to the steering-wheel angle are shown in the bottom plot of Figure 9. Much more consistent performance is obtained, undoubtedly

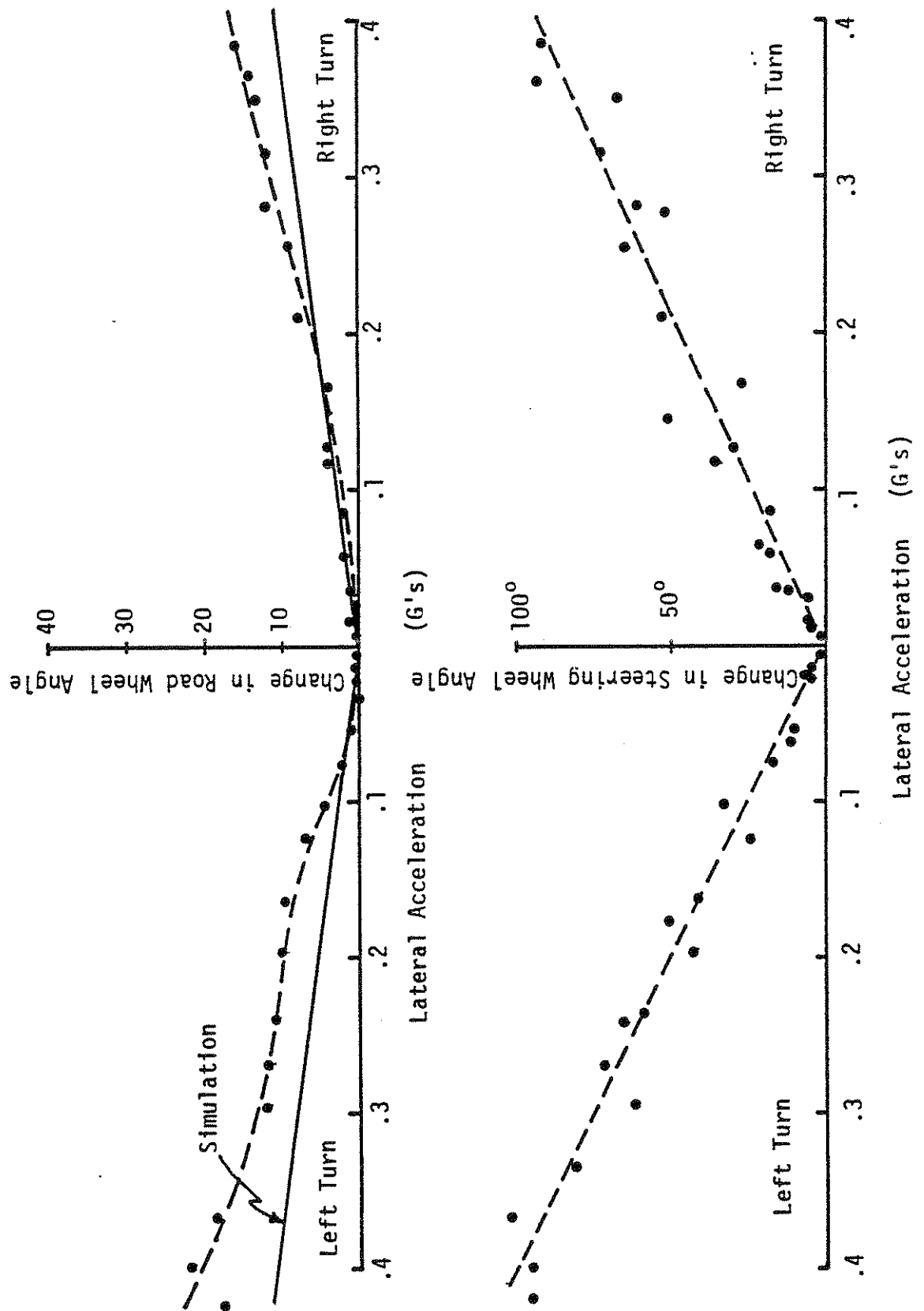


Figure 9 Empty Truck Understeer Characteristics.

because of much lower roll angles and less of the asymmetric roll steer effects. This data provides a good opportunity to assess the typical steering compliance effect on understeer gradient. The measured road wheel understeer gradient is nominally 4.25 deg/g. The steering wheel understeer gradient of 250° sw/g, when corrected for the 37 to 1 steering ratio measured in calibration, results in 6.75 deg/g. Thus it is seen that the effect of roll steer and steering system compliance is approximately 2.5 deg/g of understeer on this vehicle.

The steady-state cornering tests also provided the opportunity to evaluate the simulation's ability to predict sprung mass roll effects. The test vehicle roll angle was determined by integrating the roll rate signal at the end of the steady-state cornering test as the vehicle was returned to a straight path. The lateral acceleration was determined from the recorded yaw rate and velocity. Figure 10 shows the loaded test vehicle roll characteristics obtained from a best-fit straight line through the test data points. Shown also is the roll characteristic for the simulation obtained by noting the roll angle-lateral acceleration in the steady-state turning simulations. Reasonable agreement is obtained. It is considered doubtful that the difference indicates any error in the simulation model, but rather is the result of experimental error in the measurements and probable error in knowledge of the exact vehicle characteristics for input to the simulation.

### 5.3 Transient Maneuvers

Tests of the simulation's validity at predicting transient performance were made by comparing results in a series of step-steer maneuvers.

The vehicle maneuvers were accomplished by allowing the vehicle to achieve a straight-ahead steady-state condition as it entered the skid pad and then turning the steering wheel up against the limiter at the maximum rate possible. A step-steer effect was achieved.

In simulation of these maneuvers, the comparable approach is to input a road-wheel steer angle equivalent to the step steer, allowing the simulation to duplicate the roll steer effects associated with the roll dynamics of the vehicle.



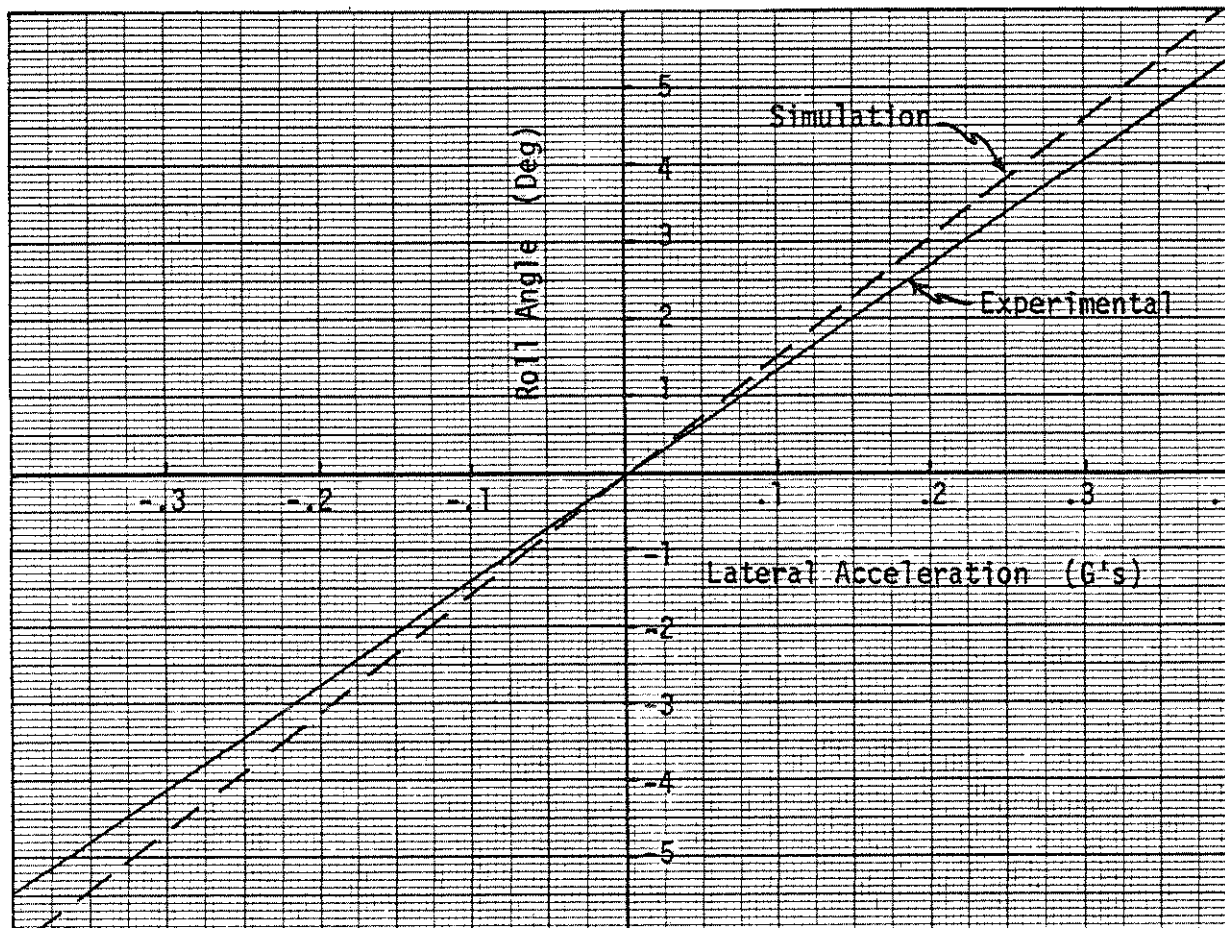


Figure 10 Comparison of Experimental and Simulation Vehicle Roll Characteristics.

Figures 11 and 12 show the comparison of time histories for steer angle, yaw rates, and roll angles for the loaded vehicle in sub-limit and limit level right-hand turns. In the steer angle plot, the top line represents the step-steer input to the road wheels in the simulation, the "simulation steer angle" represents the steer angle adjusted for roll steer effects, and the bottom line shows the experimentally measured steer angle. The divergence of the experimentally measured steer angles from the simulation cannot be explained by the measured roll steer effects; however, the experimental road-wheel steer angle was measured relative to the axle and the axle can steer as well as bend during such severe maneuvers, with the potential for errors in measurement of the steer angle. Since the simulation is in such close agreement with the vehicle performance in yaw rate and roll angle, this difference was disregarded as an error in measurement.

Figures 13 and 14 show similar comparisons in a left-hand turn. For the sub-limit case of Figure 13 very good agreement is obtained. Figure 14 represents a limit maneuver with the vehicle going yaw divergent (i.e., beginning to spin out). The simulation's predictions of the instability are qualitatively correct, differing only in the rate at which the divergence occurs. Note that the simulation reaches the point where rollover begins (inside rear wheel leaves the ground) at approximately the same magnitude of roll angle and yaw rate as the maximums achieved in testing, which was terminated as the vehicle began to roll.

Additional simulation runs were made to examine the sensitivity of yaw divergence rate to the test variables of speed and steer angle in order to explain the difference in divergence rates seen in Figure 14. Figure 15 shows the influence on yaw rate of three steer angles and a two miles per hour decrease in assumed test speed. Both factors clearly have a strong influence on yaw divergence rate, indicating that errors in the experimental measurements defining the test conditions could readily account for the observed differences in yaw rate.

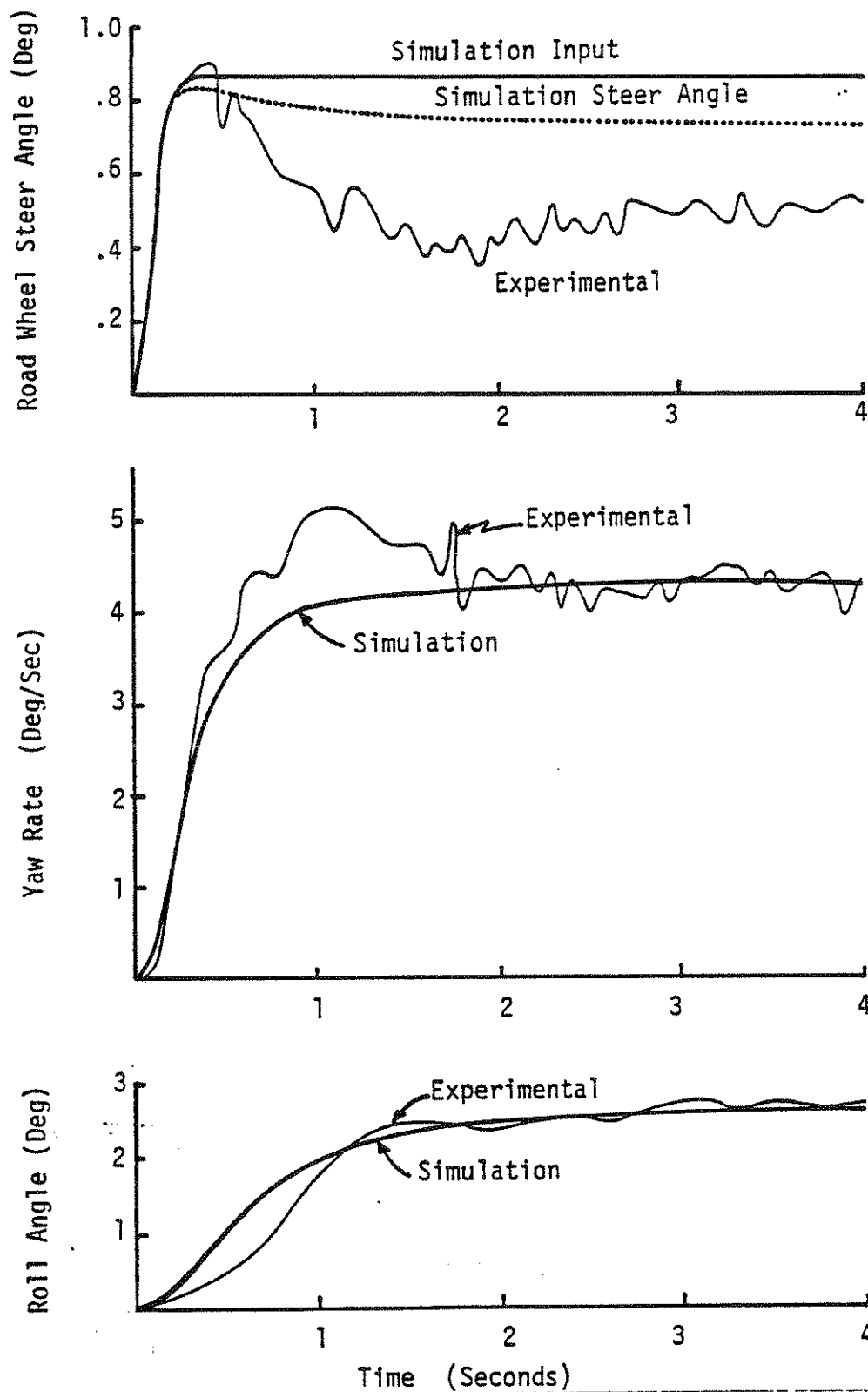


Figure 11 Time History of 50 MPH Sublimit Step Steer, Loaded Vehicle, Right Turn.

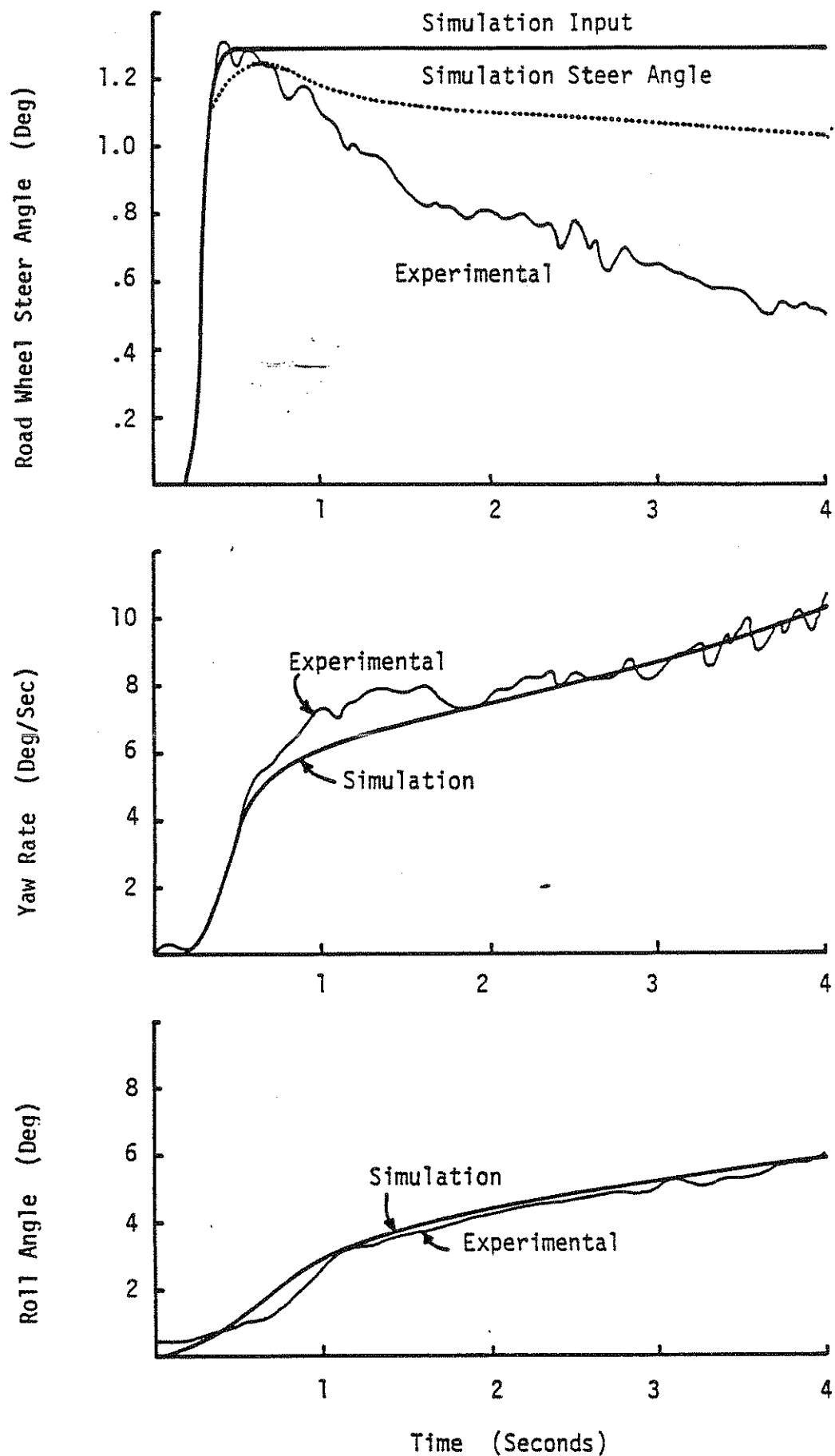


Figure 12 Time Histories of 50 MPH Limit Step Steer, Loaded Vehicle, Right Turn

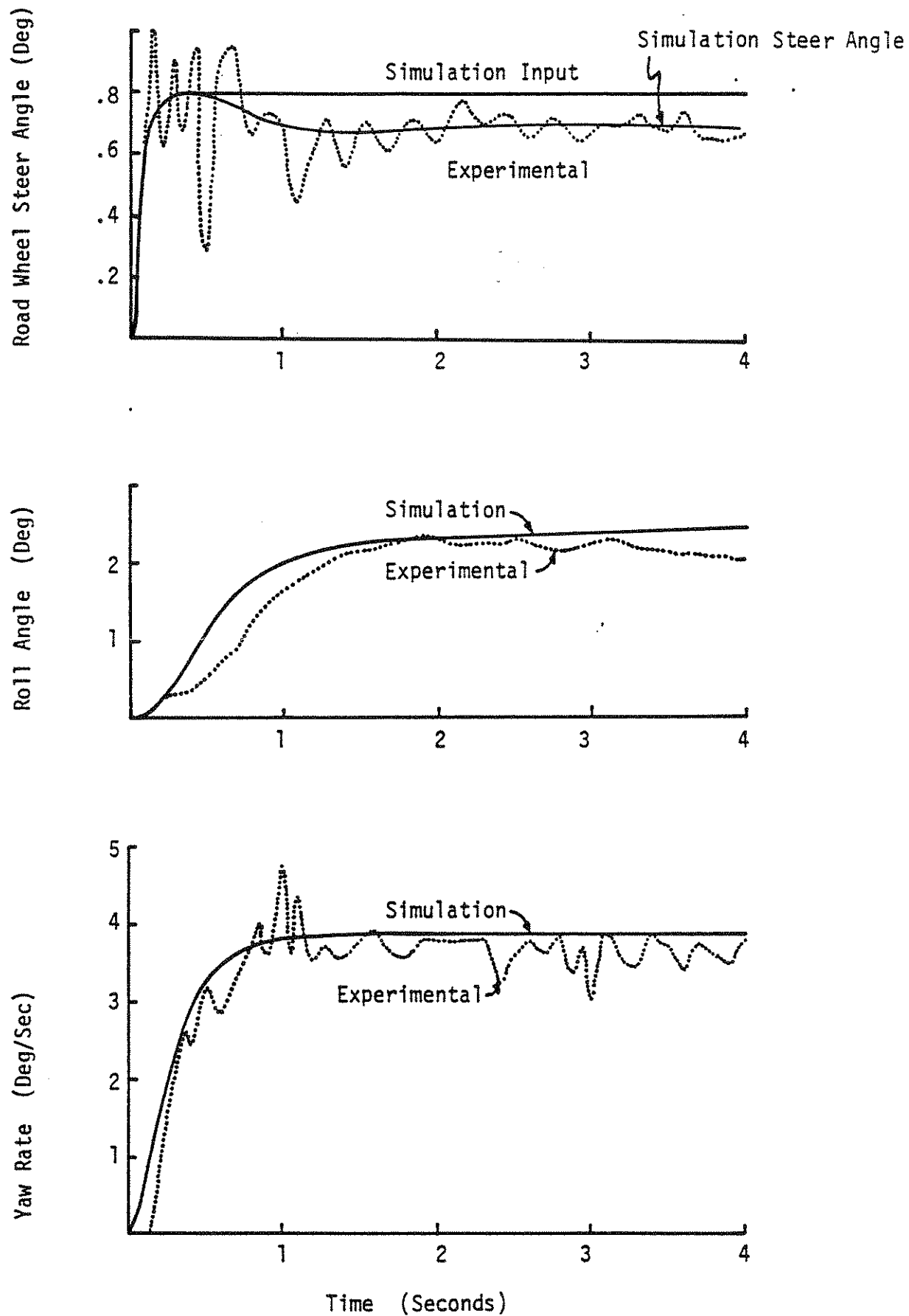


Figure 13 Time Histories of 50 MPH Sublimit Step Steer, Loaded Vehicle, Right-hand Turn

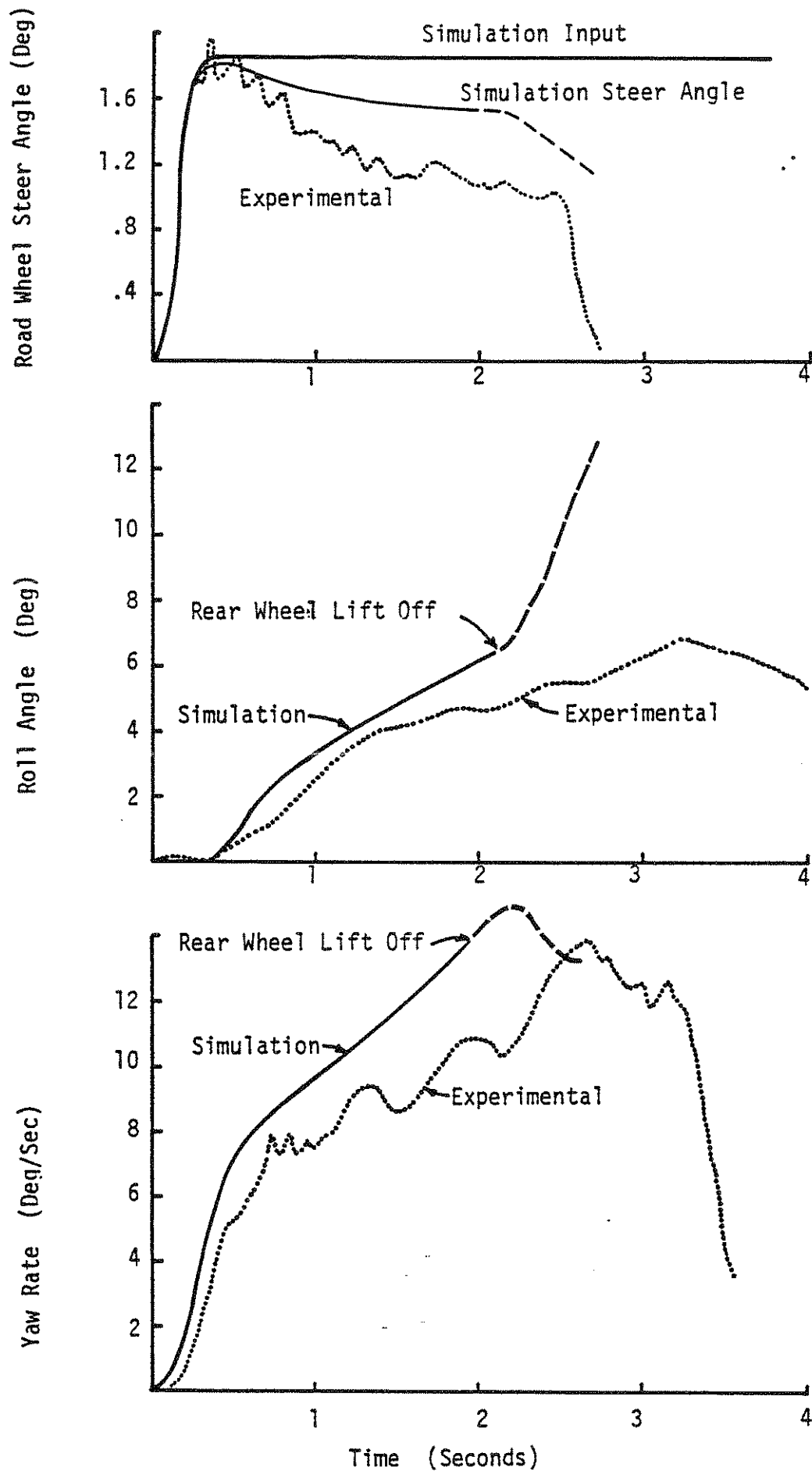


Figure 14 Time Histories of 50 MPH Limit Step Steer, Loaded Vehicle. Lefthand Turn.

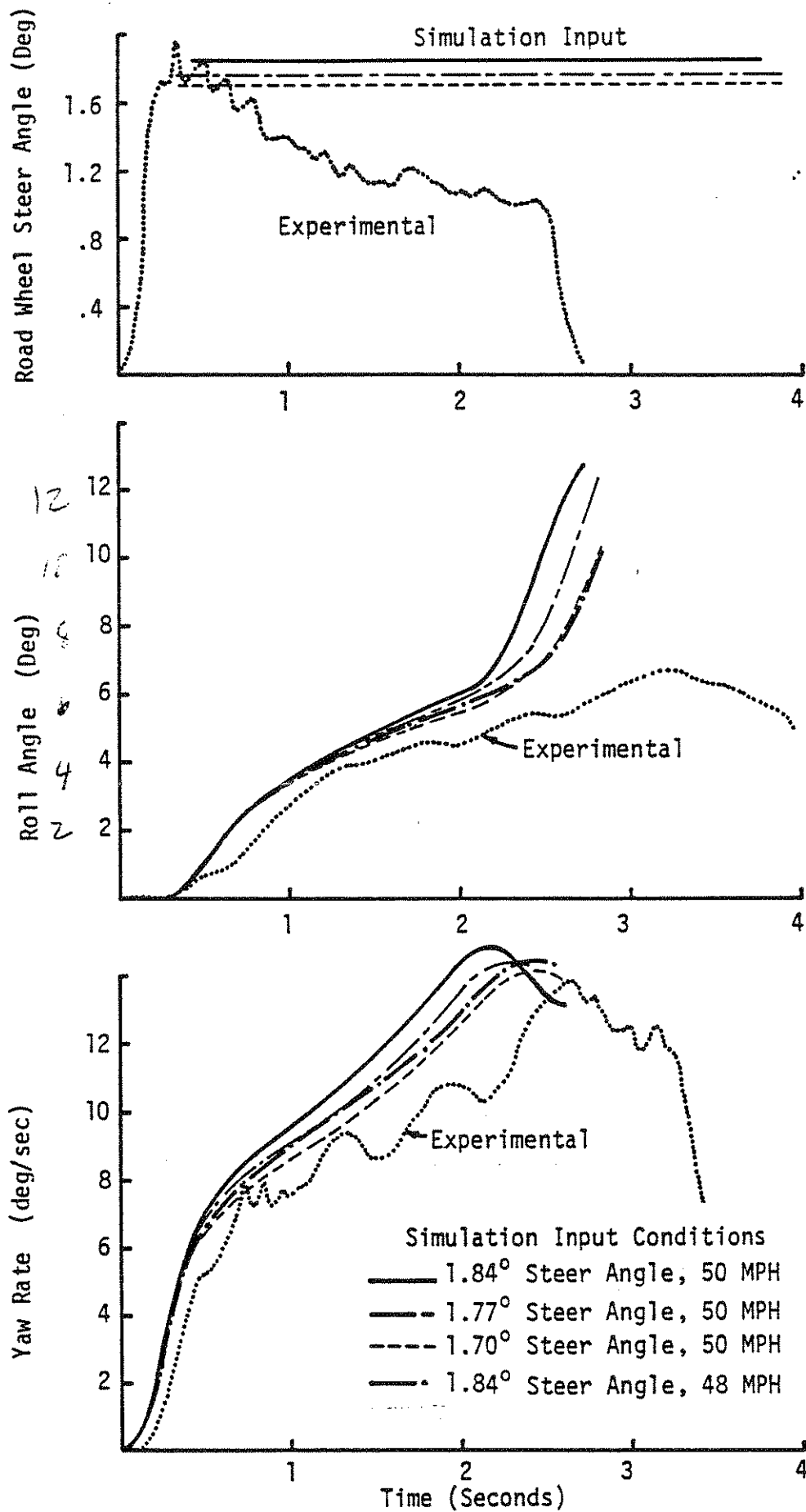


Figure 15 Influence of Test Variables on Simulation Response.

In the Figures 11 through 15 shown so far, one observes that the simulated roll angle and yaw rate may tend to lead the measured values at the beginning of a maneuver. Figure 16, which shows the measured and simulated yaw rates for a typical 20- and 50-mph step steer, demonstrates the dependence of this effect on test speed. The source of this error is the lack of modeling of tire relaxation length effects in the simulation. In the simulation, tire lateral forces are determined from instantaneous slip angle conditions, whereas on an actual vehicle it is recognized that a tire must roll some distance to achieve the lateral deflection which is prerequisite to producing a lateral force. This phenomenon, characterized by the term "tire relaxation length," results in a delay in the build-up of lateral force equivalent to approximately one-third of a wheel revolution. At 50 mph, this means a delay of approximately 0.04 second and at 20 mph, 0.1 second, the approximate delay magnitudes seen in Figure 16. The consequence of this shortcoming in the model is usually minor as long as it is recognized by the user.



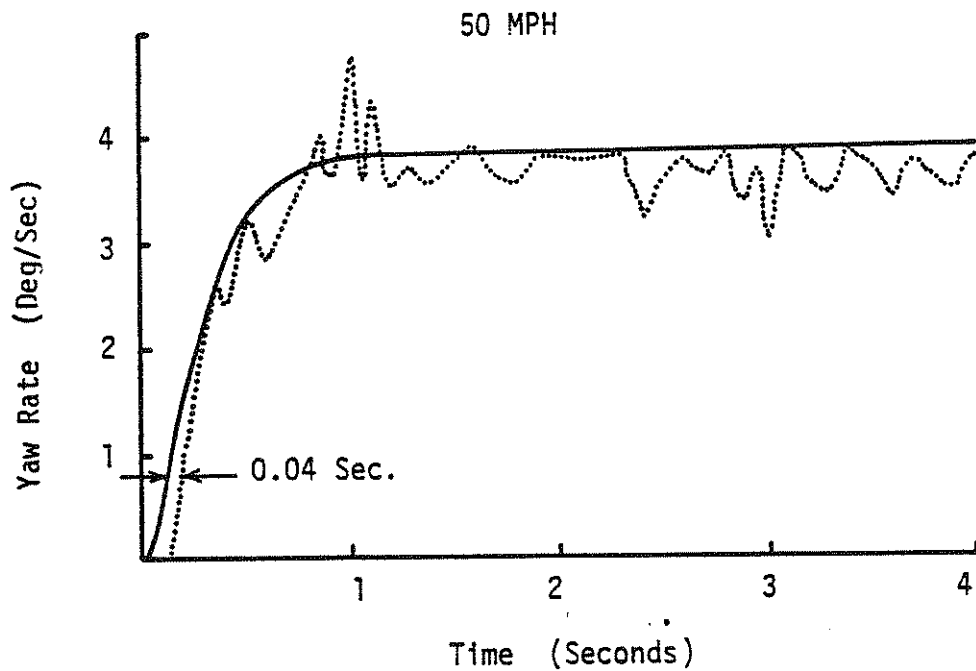
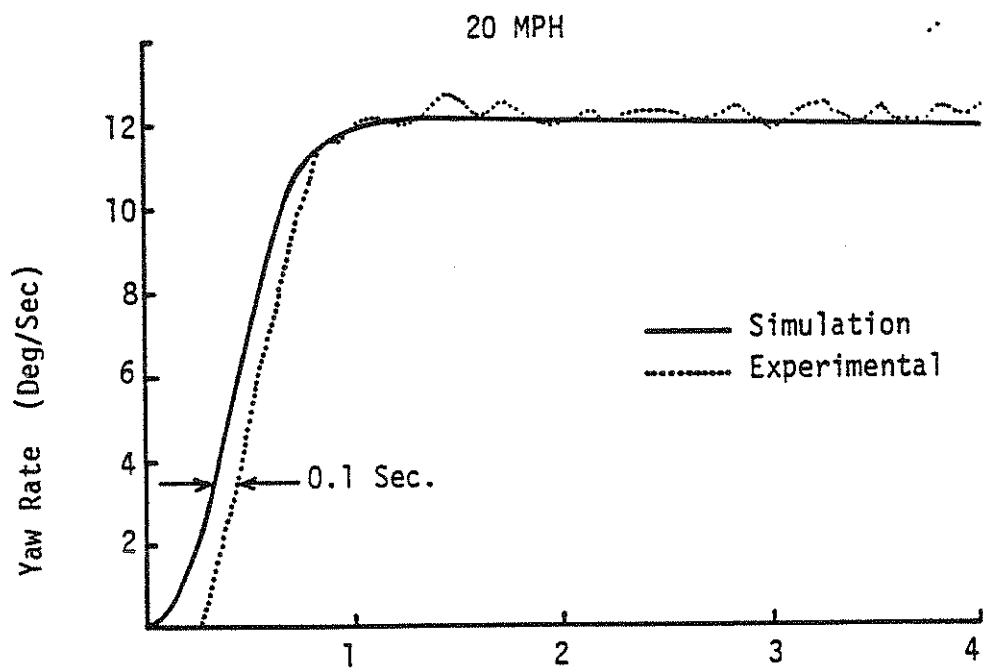


Figure 16 Yaw Rate Time Histories of 20 MPH and 50 MPH Step Steers.

## 6.0 CONCLUSIONS AND RECOMMENDATIONS

In total, the results of this validation study are positive, demonstrating that the Phase II straight truck directional response simulation is capable of duplicating the response of an actual vehicle. That conclusion is subject to the following three conditions:

- 1) The significant vehicle parameters required for program input must be accurately determined.
- 2) The validity can only be assured for the motion variables measured and compared.
- 3) The program output must be interpreted knowledgeably.

The need for the accuracy in the input description of a vehicle is very critical when a validation is being performed. As seen in Figure 15, normal experimental errors in speed or steer angle can significantly influence the apparent agreement obtained. In the process of validation, an iterative process is often involved as the first comparisons of simulation and test reveal unexpected differences, which, when examined, are traced to inaccuracies or errors in the experimental measurements or program input. Fortunately, the usefulness of these simulation programs are not dependent on every user going through the same process. In most applications, the user can assume, for example, a given tire characteristic and investigate directional response with that tire, knowing that it is typical, but yet, not precisely equivalent to any specific tire on hand. Much of the utility of computer simulation programs derives not from absolute prediction of a certain vehicle/test maneuver situation (as required for validation), but as a tool for studying generalized performance and sensitivity of performance to the vehicle parameters.

The statement limiting validity to only the measured and compared motion variables is made to stress to the reader that validation is based on comparison of the overall vehicle performance. The simulation

necessarily calculates and puts out a number of other variables (accelerations, tire conditions, etc.) which, by implication, must be systematically correct, but when compared on a point-for-point basis may not appear as accurate as the results shown here. Hence, in use of the program, the user must be aware and informed as to the degree of accuracy to be expected with each of the many motion variables.

The last condition expands on this notion that the output of the simulation program must be interpreted knowledgeably. As discussed in the previous sections, the directional response simulations do not model tire relaxation length effects, nor is the simulation as complete as may be desired in modeling the steering system between the steering wheel and road wheels. Hence, the use of the simulation's response predictions is only valid when these shortcomings are recognized and the results are interpreted appropriately.

Considering the utility of the directional response simulations, and recognizing that vehicles are directionally controlled by inputs at the steering wheel, it is recommended that more thorough modeling of the steering system be considered. Such a model would add to the overall utility of the directional response programs by allowing investigation of steering-system performance characteristics as they influence handling, and at the same time, would allow program operation by specification of steering-wheel input which is more closely associated with the actual operation of a vehicle. It is clear from the loaded truck tests that the steering system itself plays a vital role in the handling characteristics of heavy trucks.

## 7.0 REFERENCES

1. Murphy, R.W., Bernard, J.E., and C.B. Winkler, "A Computer-Based Mathematical Method for Predicting the Braking Performance of Trucks and Tractor-Trailers." Phase I Report, Motor Truck Braking and Handling Performance Study, Univ. of Michigan, Highway Safety Research Institute, September 15, 1972.
2. Winkler, C.B., Bernard, J.E., Fancher, P.S., MacAdam, C.C., and T.M. Post, "Predicting the Braking Performance of Trucks and Tractor-Trailers." Phase III Technical Report, Truck and Tractor-Trailer Braking and Handling Project, Univ. of Michigan, Highway Safety Research Institute, June 1976.
3. Bernard, J.E., Winkler, C.B., and P.S. Fancher, "A Computer-Based Mathematical Method for Predicting the Directional Response of Trucks and Tractor-Trailers." Phase II Technical Report, Motor Truck Braking and Handling Performance Study, Univ. of Michigan, Highway Safety Research Institute, June 1, 1973.
4. Bernard, J., Starr, D., and R. Gupta, "Programs for Estimating Inertial Properties of Trucks and Trailers." Univ. of Michigan, HSRI, August 9, 1973.
5. "Survey of Single-Axle Steering and Suspension Properties - MVMA Project #1.31", Motor Truck Braking and Handling Program. Third Quarterly Report, (January 1977 - March 1977).
6. R.D. Ervin, "Measurement of the Longitudinal and Lateral Traction Properties of Truck Tires." Proceedings of a Conference on the Braking of Road Vehicles, Inst. of Mech. Engrs., Loughborough Univ. of Technology, March 23-25, 1976.
7. Fancher, P.S., Winkler C.B., MacAdam, C.C., Segel, L., and C. Mallikarjunarao, "Steering Controllability Characteristics." Final Technical Report. Univ. of Michigan, HSRI, August 1977.
8. T.D. Gillespie, "Front Brake Interactions with Heavy Vehicle Steering and Handling During Braking." SAE Paper No. 760025, February 1976, 16 pp.
9. Gillespie, T.D., and C.B. Winkler, "On the Directional Response Characteristics of Heavy Trucks." Presented at 2nd IUTAM Symposium on Dynamics of Vehicles on Roads and Tracks, Vienna, September 19-23, 1977.

APPENDIX A

COPY OF:

"SURVEY OF SINGLE-AXLE STEERING AND SUSPENSION PROPERTIES -  
MVMA PROJECT 1.31"

Third Quarterly Report, January-March 1977

Survey of Single-Axle Steering and Suspension Properties -  
MVMA Project #1.31

The Single-Axle Suspension Measurement Facility (SASMF) has been completed and has been exercised using the International Harvester highway tractor owned by HSRI. The vehicle is shown in position for testing in Figure 1.

As can be seen in Figure 1, the test vehicle's frame is rigidly attached to the fixed frame of the facility during testing. The suspension is then exercised by vertically-oriented hydraulic cylinders located beneath each front wheel. The left side vertical cylinder is just visible in Figure 2. Normal loads on the tires are transduced by load cells (not visible in Figure 2) located atop these cylinders, and restrictions on contact patch motion in the ground plane are eliminated by hydrostatic bearings seen in Figure 2 to be located immediately beneath the wheels. Tire shear forces and moments are also generated by horizontally-oriented cylinders acting on the upper element of the hydrostatic bearings. Forces and moments so produced are transduced by load cells located on the cylinder rods. Also visible in Figure 2 is one of the potentiometric road wheel steer angle transducers. In Figure 1, the string potentiometer used to transduce vertical wheel spindle position is also visible.

The tractor employed as a test vehicle has been used by the Institute until recently as the base vehicle for our Mobile Tire Tester (passenger car tires). Measurements of the following properties were made on the front suspension and steering system.

1. Vertical spring rates and hysteretic (Coulomb friction) characteristics.
2. Roll stiffness and hysteretic properties.
3. Roll center position.
4. Roll steer properties.

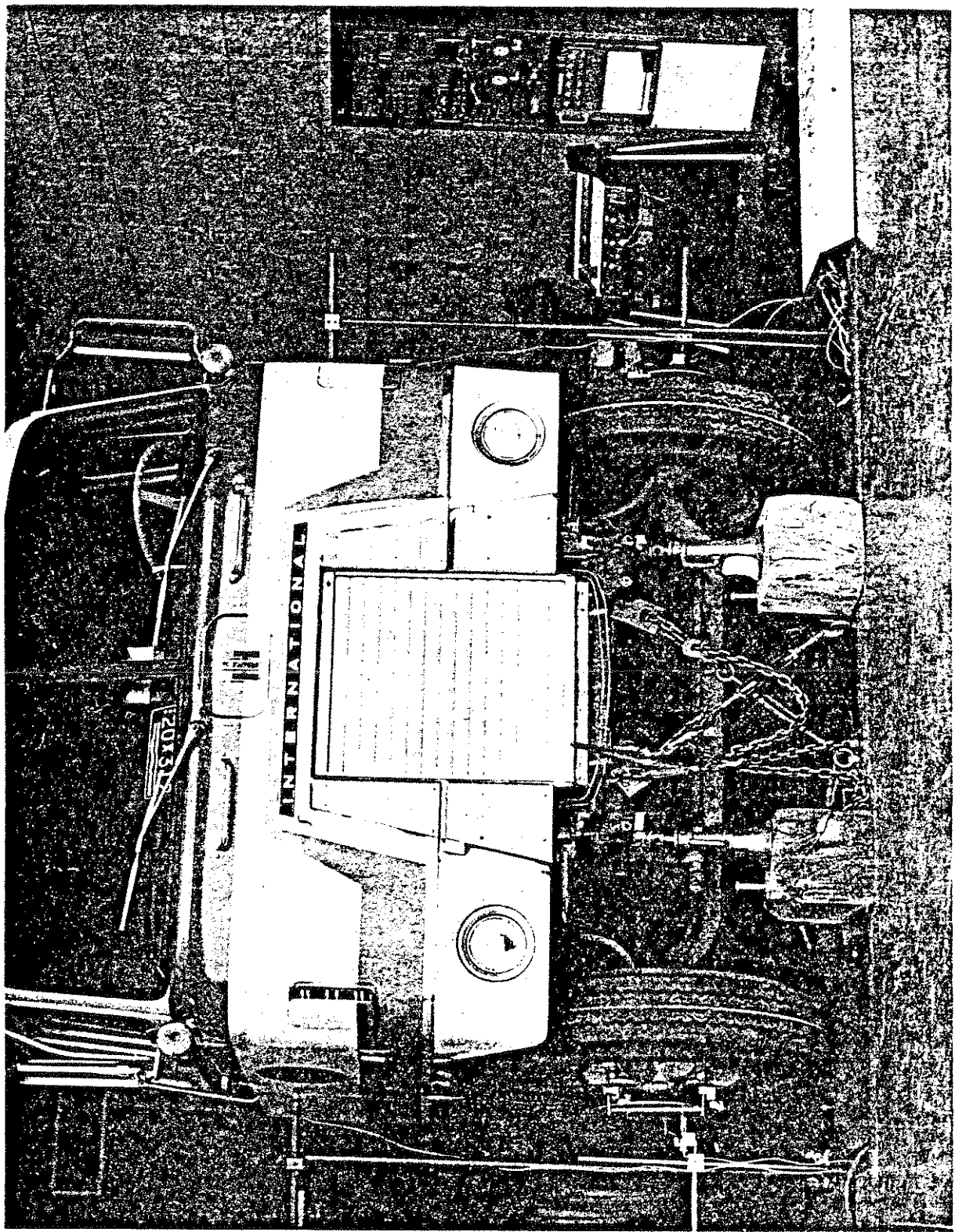


Figure 1. Test vehicle in position.

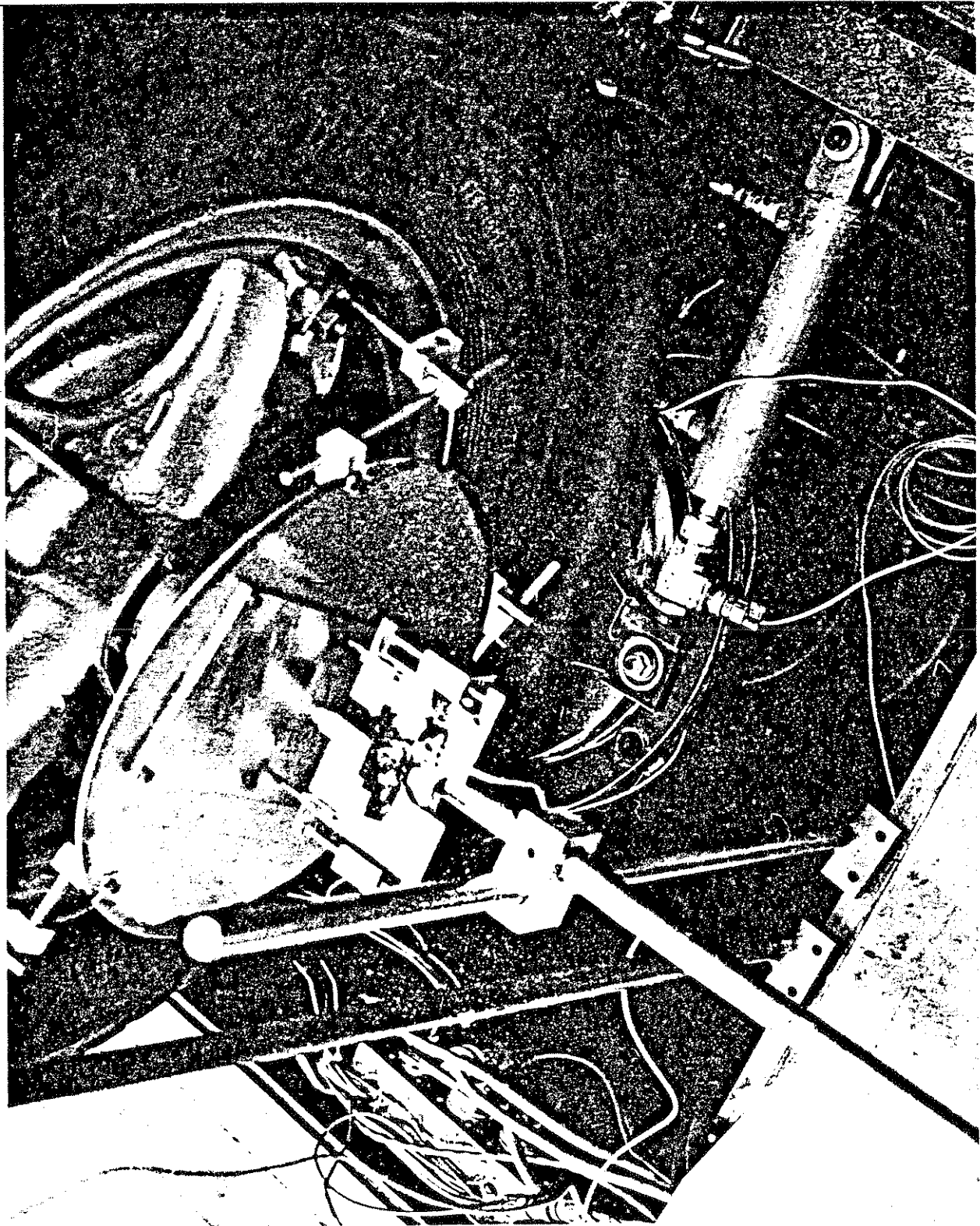


Figure 2. Left front wheel station.



5. Bounce steer properties
6. Compliance steer response to aligning moment.
7. Compliance steer response to brake force.
8. Overall steering ratio.

A brief review of the parameter data gathered appears in Figures 3 through 10.

The data displays some interesting qualities. First, there is substantial asymmetry between left- and right-hand springs. Their rates are different as are the levels of compressive force required to contact the bump stops. This behavior may result in part from the previous use of this vehicle. As a mobile tire tester, it spent a great deal of time traveling a counter-clockwise oval course on various test tracks.

The roll rate data indicates that there is a substantial amount of "auxiliary roll stiffness" present in the suspension, even though no anti-sway bar is present. Based on a simple model of two vertical springs acting on the solid axle at the 32-inch lateral spacing, the spring rate data would predict a suspension roll stiffness of 9050 in-lb/deg.\* Measuring roll stiffness directly, a value of 13,070 in-lb/deg\* was found. The 4000 in-lb/deg of auxiliary roll stiffness is readily explained by the torsional stiffness of the individual leaf springs when subjected to rotations about their longitudinal axis because of the relative roll motion of axle and frame (see Figure 11). Formulations presented by Timoshenko [1] predict that this level of auxiliary roll stiffness could derive almost completely from the torsional flexing of the upper leaves alone. Additional stiffening by the leaf stack and softening by the shackles, brackets, frames, and bearings apparently offset one another.

---

\*These quantities are based on spring rates for large deflections about a nominal axle load of 8000 lb.

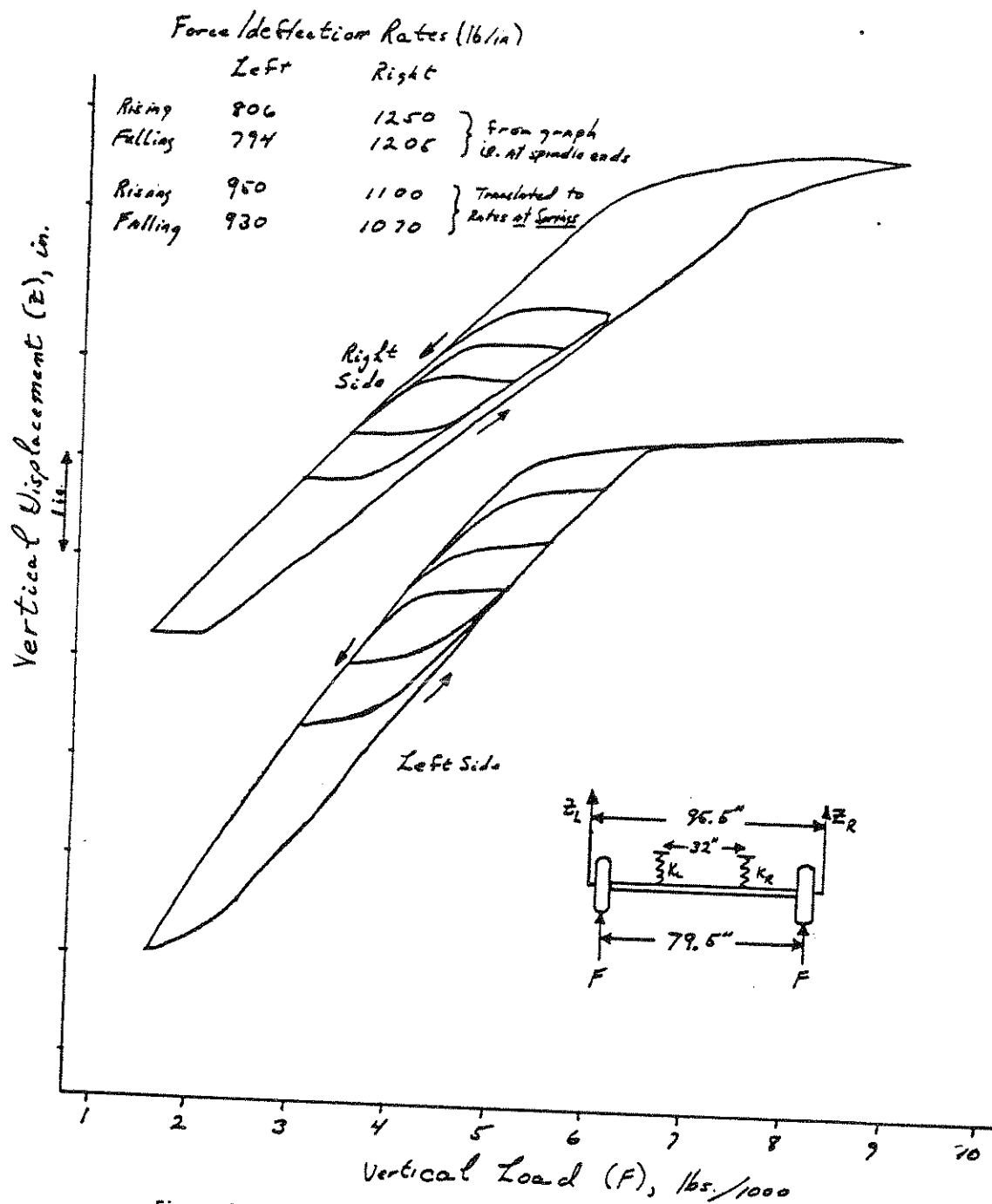


Figure 3. Vertical spring rate and hysteretic characteristics.

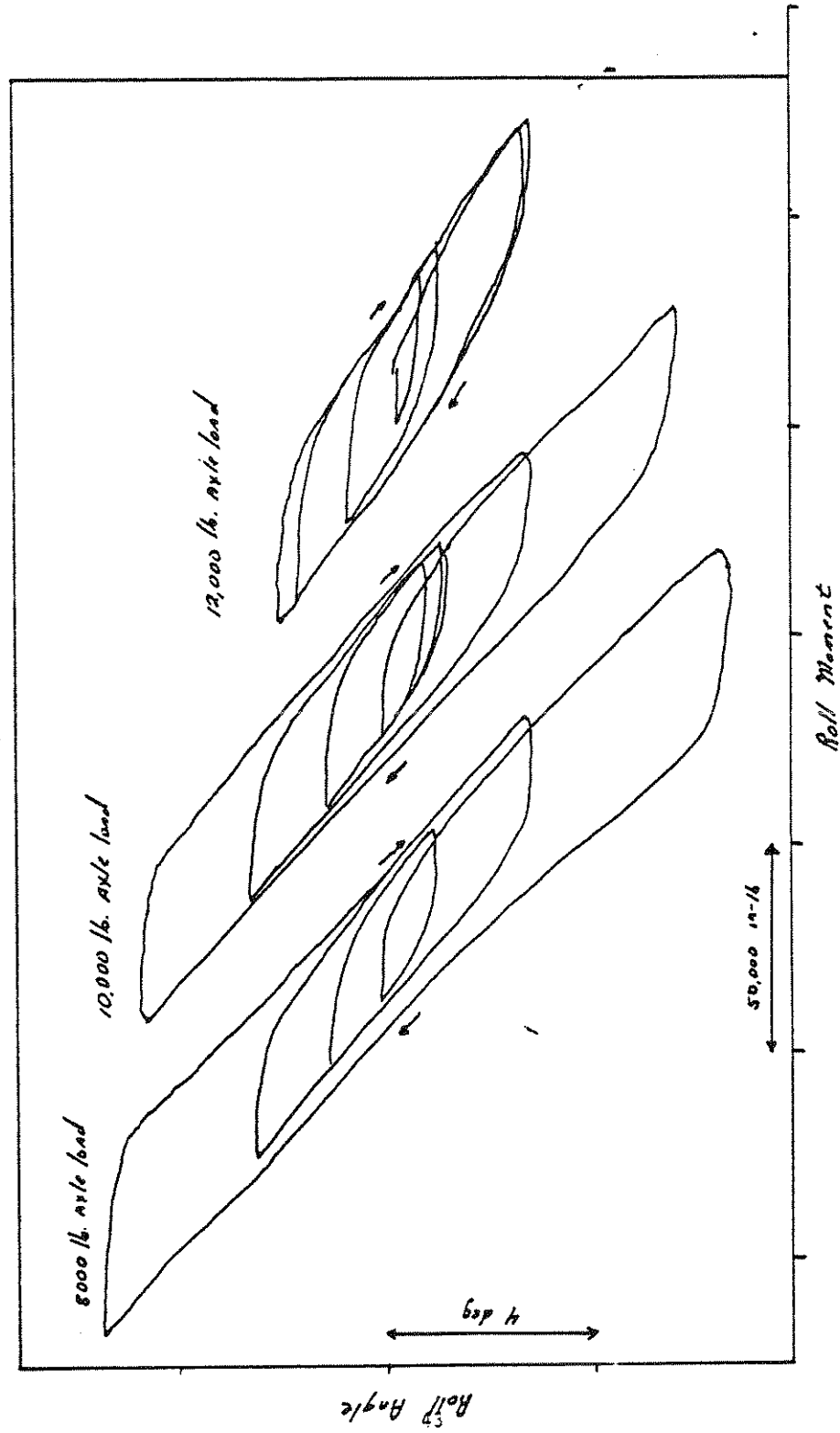
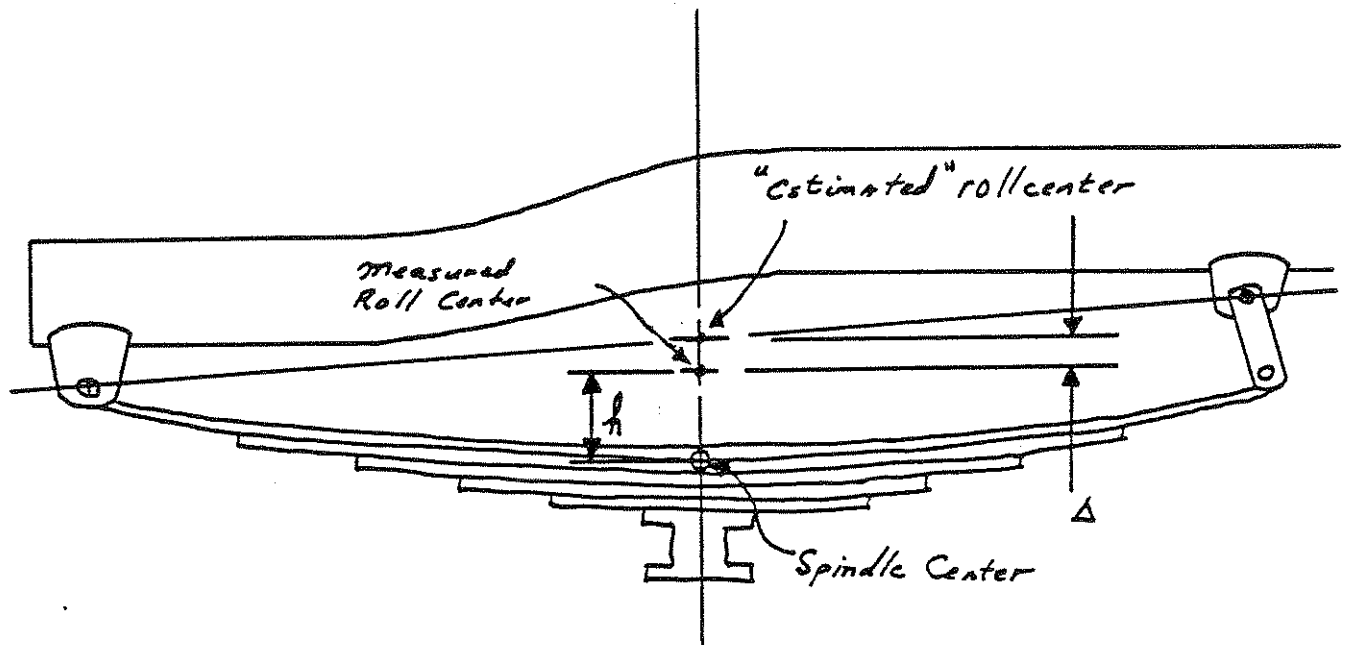


Figure 4. Roll stiffness and hysteretic characteristics at three constant axle loads.



Axle load, lb.	$\Delta$ , in	$h$ , in.
8000	0.90	5.35
9000	1.26	4.50
10,000	0.88	4.25
11,000	.76	3.75
12,000	2.01	1.77

Figure 5. Roll center position.

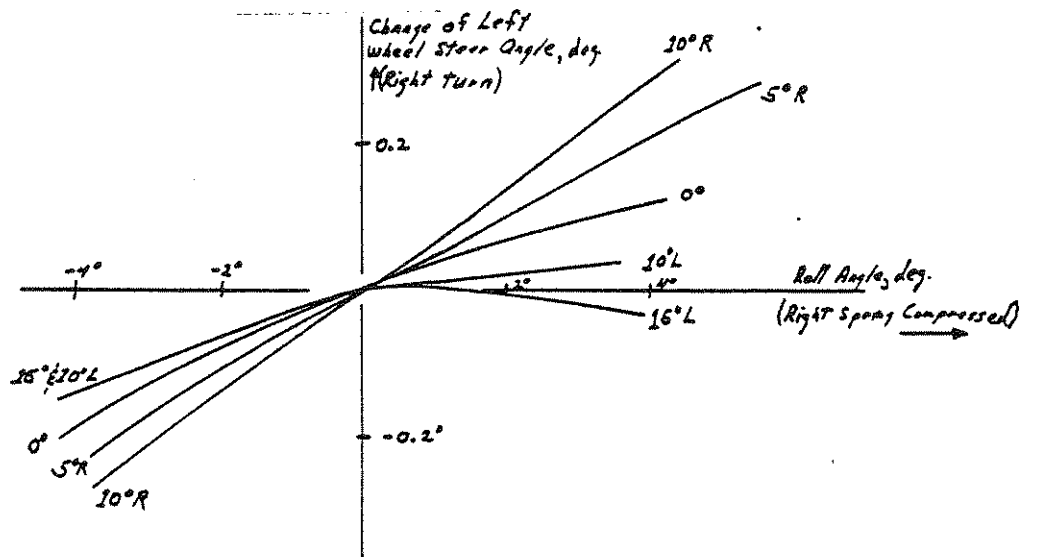


Figure 6. Roll steer characteristics as a function of nominal steer angle; 10,000 lb. axle load.

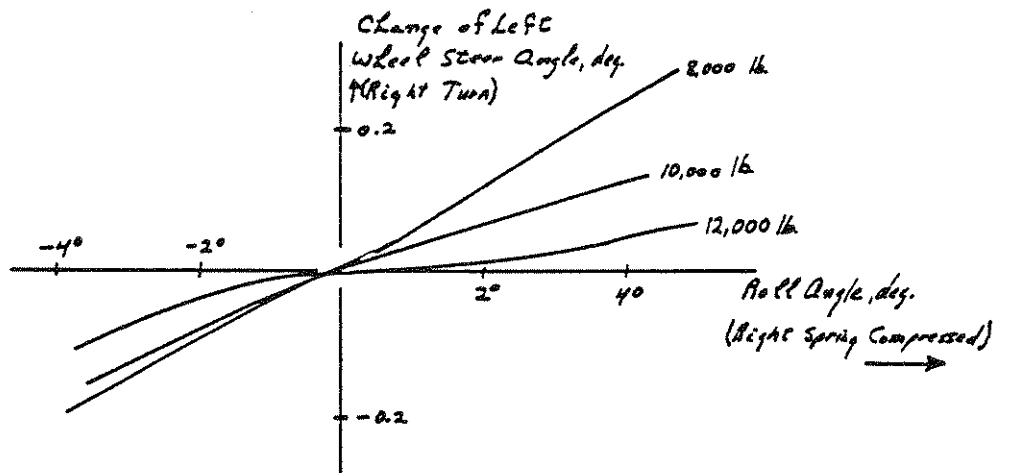


Figure 7. Roll steer characteristics as a function of axle load; 0° nominal steer angle.

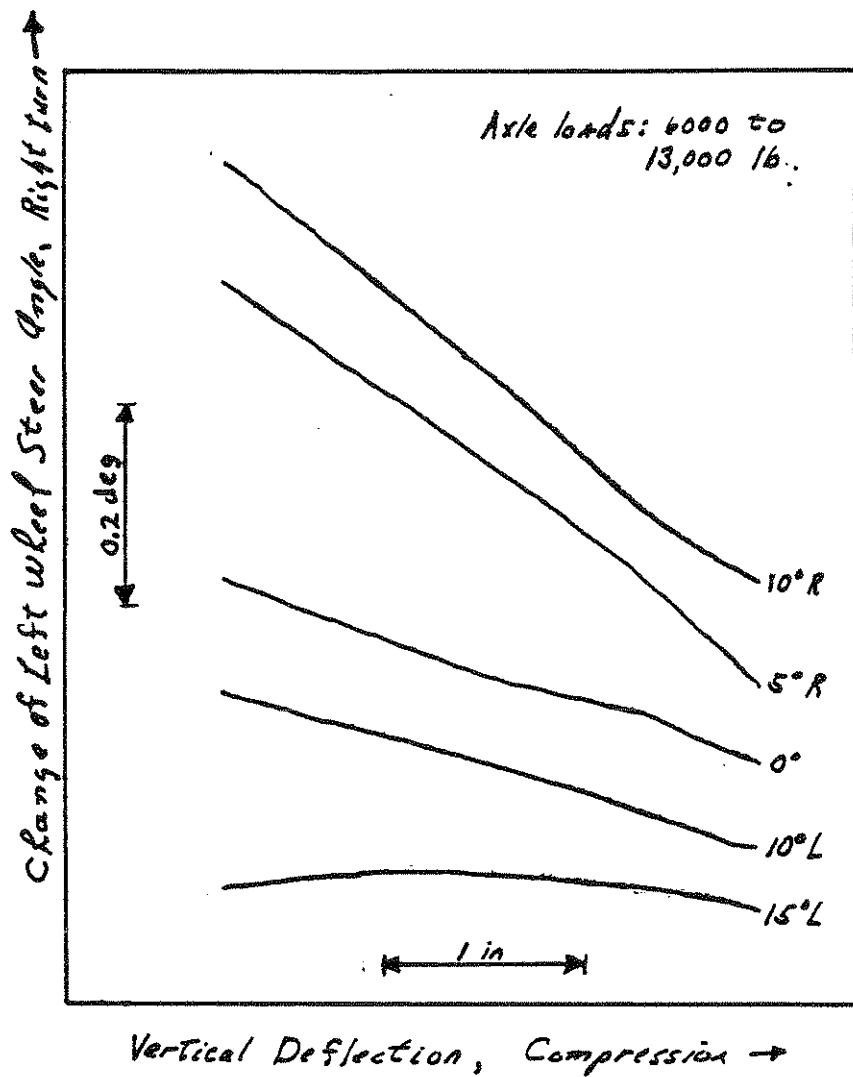


Figure 8. Bounce steer characteristics as a function of nominal steer angle.

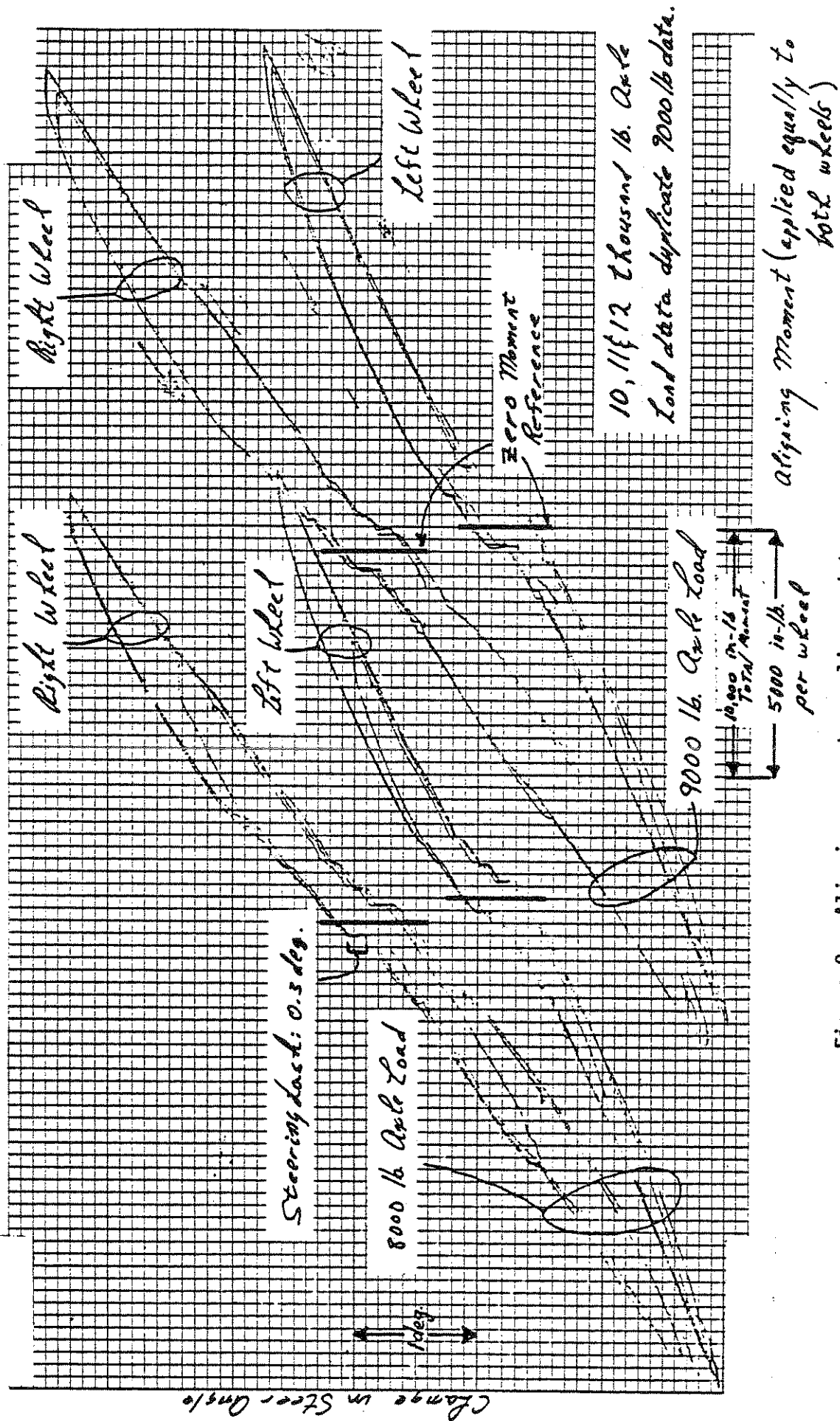
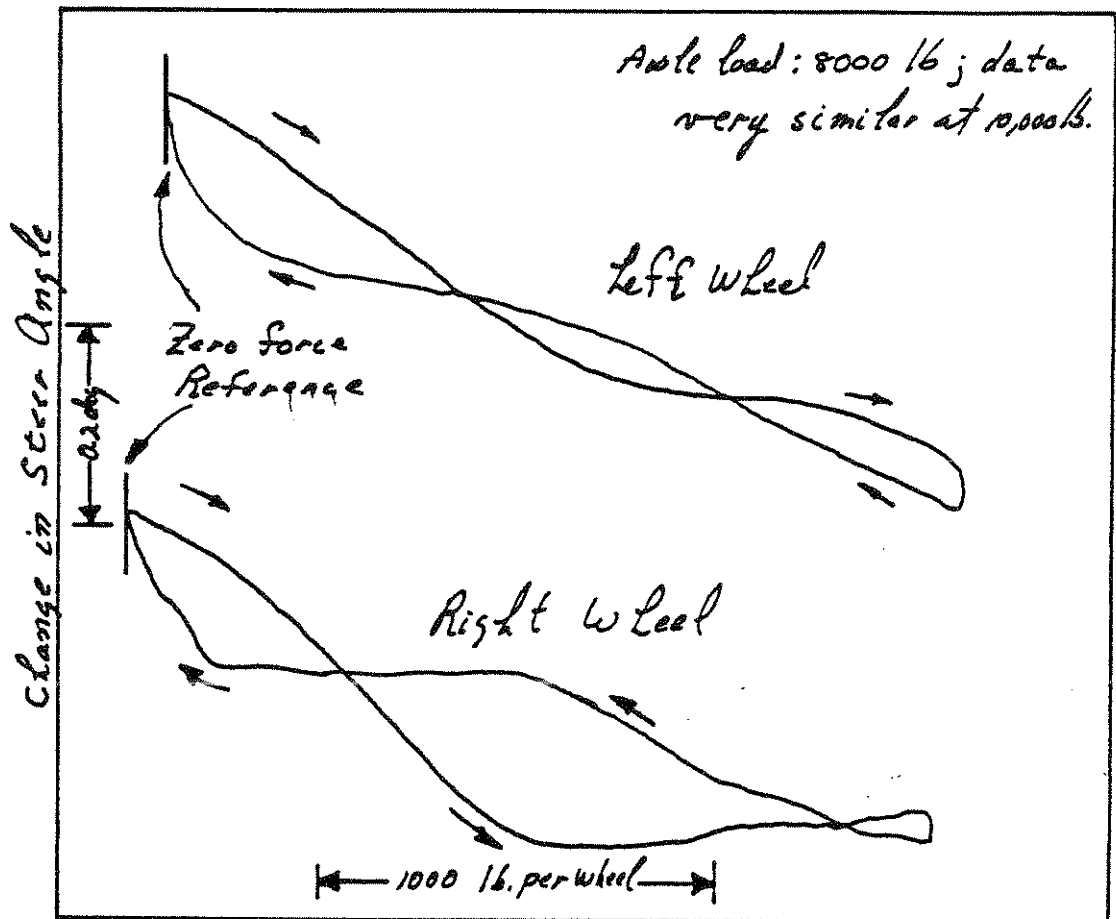


Figure 9. Aligning moment compliance data.



Brake Force applied equally to each wheel  
 Figure 10: Brake force compliance data.



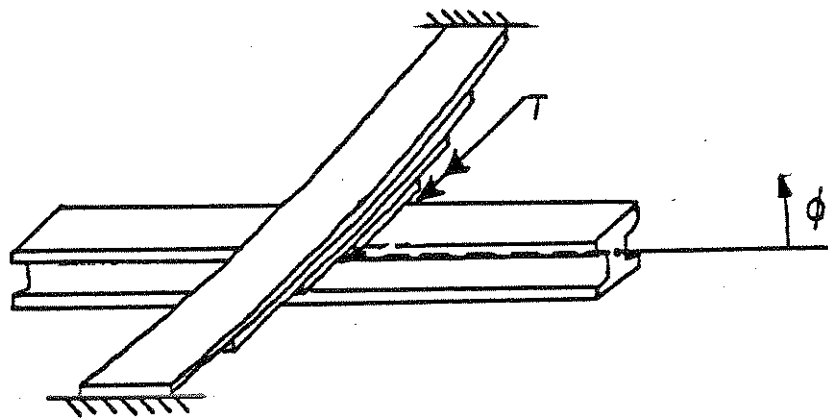


Figure 11. Auxiliary roll stiffness can derive from lengthwise twisting of the springs.

The roll center position, as measured, was found to be slightly below the position which Cole [2] estimates for solid axles located by leaf springs (see "estimated roll center" in Figure 5). Considering the level of Coulomb friction present in the suspension, the consistency of this measurement for different axle loads is somewhat surprising.

Roll steer (degrees steer/degrees roll) was found to be a strong function of nominal steer angle as well as axle load and roll angle (Figures 6 and 7). Bounce steer (degrees steer/inches of axle bounce) was also found to be a strong function of nominal steer angle (Figure 8).

Figure 9\* shows the reactions of the steering and suspension system to aligning moment. In these tests, equal moments were applied to both wheels simultaneously. The slope of the left wheel trace (based on total moment) indicates the compliance of the steering column, gearbox, and drag link mechanism. The difference in slopes (based on "per wheel" moment) of the right and left wheel traces is the compliance of the tie rod assembly. Steering system lash also appears clearly in this data\*\*. Note that, while lash appears small in Figure 9, it is of a magnitude which represents a large portion of total steering deflection in Figures 6, 7, 8, and 10.

Figure 10 shows steering reaction to applied brake force. This behavior essentially results from geometry changes associated with leaf spring wrap-up, rather than from true compliance of the steering system.

---

\*This figure is a direct photocopy of the X-Y plotter recording. In all other figures we have presented tracings of X-Y plotter recordings to improve legibility.

\*\*Lash had been adjusted to a minimum in the ball joints. Most of the lash shown in the figure is in the gearbox.

Partly as a result of experienced gained during this initial test activity, several modifications are being made to the SASMF to enhance its operational characteristics. Following this activity, measurements will be made on additional vehicles. We expect to be requesting test vehicles of member companies in the near future.

#### References

1. Timoshenko, S., Young, D.H., Strength of Materials. D. Van Nostrand Company, Inc., Princeton, N.J., 1962.
2. Cole, D.E., Elementary Vehicle Dynamics. Dept. Mech. Eng., Univ. of Michigan, Ann Arbor, September 1971.

APPENDIX B  
TEST VEHICLE DATA INPUT LIST

LOADED IHC TRACTOR 50MPH SEP19 1978,SIMULATION OF RUN

02	KEY
24.0	AA1
24.0	AA2
1.0	AA4
1.0	AA5
0.	AA6
0.	AA7
0.	AA8
61.42	A1
80.58	A2
20.3	ALPHA1
20.3	ALPHA2
0.25	AN1
0.25	AN1
0.25	
10.0	C1
20.0	C2
10.0	C3
20.0	C4
-1.	CALF
500.	CF1
100.	CF2
40000.	CS1
40000.	CS2
40000.	CS3
27.6	DELTA1
13.0	DT2
.006	FA1
.006	FA2
.006	FA3
33852.	IXX
120000.	IYY
120000.	IZZ
0.0	IXZ
5307.	JA1
11088.	JA2
244.6	JS1
393.2	JS2
393.2	JS3
1012.5	K1
3000.	K2
4000.	KRS1
0.	KRS(2)
78000.	AKRS
5700.	KT1
5700.	KT2

5700.	KT3
-1.	SIDE-TO-SIDE KEY
-1.	MUZERO KEY
24907.	PW
7485.	PJ1
50896.	PJ2
54422.	PJ3
6.	PX
70.25	PY
24.55	RCH1
22.0	RCH2
0.0	RS1
0.05	RSC1
0.10	RSC2
16.0	SY1
17.5	SY2
2.8	TIMF
40.25	TRA1
36.0	TRA2
73.333	VEL
13893.	W
1190.	WS1
2340.	WS2
2170.	WS3
0.001,0.001	TQ
0.001,0.001	TQ
0.001,0.001	TQ
0.001,0.001	TQ
0.001,0.001	TQ
0.001,0.001	TQ
02	TIME/PRESSURE
0.0,0.0	
10.0,0.0	
02	PRESSURE/TORQUE
0.0,0.0	
0.0,0.0	
02	
0.0,0.0	
0.0,0.0	
02	
0.0,0.0	
0.0,0.0	
02	PRESSURE/TORQUE
0.0,0.0	
0.0,0.0	
02	
0.0,0.0	
0.0,0.0	

02

0.0,0.0

0.0,0.0

00

# ALIGNING TORQUE TABLE KEY

05

1375.,05,

0.00,0.

2.,35.

4.,31.8

8.,27.6

16.,10.

2890.,05,

0.,0.

2.,90.2

4.,114.5

8.,102.3

16.,57.

5780.,05,

0.,0.

2.,209.6

4.,301.8

8.,306.8

16.,180.

7500.,05,

0.,0.

2.,282.5

4.,419.5

8.,445.7

16.,344.

9000.,05,

0.,0.

2.,345.4

4.,533.1

8.,557.1

16.,452.

05

1375.,05,

00.,0.

2.,35.

4.,31.8

8.,27.6

16.,10.

2890.,05,

0.,0.

2.,90.2

4.,114.5

8.,102.3

16.,57.

5780.,05,  
0.,0.  
2.,209.6  
4.,301.8  
8.,306.8  
16.,180.  
7500.,05,  
0.,0.  
2.,282.5  
4.,419.5  
8.,445.7  
16.,344.  
9000.,05,  
0.,0.  
2.,345.4  
4.,533.1  
8.,557.1  
16.,452.  
05  
1375.,05,  
0.000,0.  
2.,35.  
4.,31.8  
8.,27.6  
16.,10.  
2890.,05,  
0.,0.  
2.,90.2  
4.,114.5  
8.,102.3  
16.,57.  
5780.,05,  
0.,0.  
2.,209.6  
4.,301.8  
8.,306.8  
16.,180.  
7500.,05,  
0.,0.  
2.,282.5  
4.,419.5  
8.,445.7  
16.,344.  
9000.,05,  
0.,0.  
2.,345.4  
4.,533.1  
8.,557.1



16.,452.

8, STEP STEER OF PEAK 1.84DEG

0.0,0.0

0.1,0.0

0.2,-0.1

0.3,-0.8

0.4,-1.74

0.5,-1.84

0.6,-1.84

2.8,-1.84

8,

0.0,0.0

0.1,0.0

0.2,-0.1

0.3,-0.8

0.4,-1.72

0.5,-1.84

0.6,-1.84

2.8,-1.84

06,

Tire Lateral Force Tables

0.,0.,0.5,10.

3000.,540.,0.5,10.

4500.,645.,0.5,10.

6000.,685.,0.5,10.

7500.,710.,0.5,10.

9000.,760.,0.5,10.

06,

0.,0.,0.5,10.

3000.,540.,0.5,10.

4500.,645.,0.5,10.

6000.,685.,0.5,10.

7500.,710.,0.5,10.

9000.,760.,0.5,10.

06,

0.,0.,0.5,10.

3000.,540.,0.5,10.

4500.,645.,0.5,10.

6000.,685.,0.5,10.

7500.,710.,0.5,10.

9000.,760.,0.5,10.

06,

0.,1.10

3000.,1.08

4500.,1.03

6000.,0.95

7500.,0.93

9000.,0.90

06,  
0.,1.10  
3000.,1.08  
4500.,1.03  
6000.,0.95  
7500.,0.93  
9000.,0.90

06,  
0.,1.10  
3000.,1.08  
4500.,1.03  
6000.,0.95  
7500.,0.93  
9000.,0.90

0.0

0.0

02

0.1

0

0.

G1

G2

NO WIND

TINC

NO PLOT

TRUCK